

Microcanonical unimolecular rate theory at surfaces. II. Vibrational state resolved dissociative chemisorption of methane on Ni(100)

H. L. Abbott, A. Bukoski, and I. Harrison^{a)}

Department of Chemistry, University of Virginia, Charlottesville, Virginia 22904-4319

(Received 18 December 2003; accepted 7 June 2004)

A three-parameter microcanonical theory of gas-surface reactivity is used to investigate the dissociative chemisorption of methane impinging on a Ni(100) surface. Assuming an apparent threshold energy for dissociative chemisorption of $E_0 = 65$ kJ/mol, contributions to the dissociative sticking coefficient from individual methane vibrational states are calculated: (i) as a function of molecular translational energy to model nonequilibrium molecular beam experiments and (ii) as a function of temperature to model thermal equilibrium mbar pressure bulb experiments. Under fairly typical molecular beam conditions (e.g., $E_t \geq 25$ kJ mol⁻¹, $T_s \geq 475$ K, $T_n \leq 400$ K), sticking from methane in the ground vibrational state dominates the overall sticking. In contrast, under thermal equilibrium conditions at temperatures $T \geq 100$ K the dissociative sticking is dominated by methane in vibrationally excited states, particularly those involving excitation of the ν_4 bending mode. Fractional energy uptakes f_j defined as the fraction of the mean energy of the reacting gas-surface collision complexes that derives from specific degrees of freedom of the reactants (i.e., molecular translation, rotation, vibration, and surface) are calculated for thermal dissociative chemisorption. At 500 K, the fractional energy uptakes are calculated to be $f_t = 14\%$, $f_r = 21\%$, $f_v = 40\%$, and $f_s = 25\%$. Over the temperature range from 500 K to 1500 K relevant to thermal catalysis, the incident gas-phase molecules supply the preponderance of energy used to surmount the barrier to dissociative chemisorption, $f_g = f_t + f_r + f_v \approx 75\%$, with the highest energy uptake always coming from the molecular vibrational degrees of freedom. The predictions of the statistical, mode-nonspecific microcanonical theory are compared to those of other dynamical theories and to recent experimental data. © 2004 American Institute of Physics. [DOI: 10.1063/1.1777221]

I. INTRODUCTION

Increasing interest in the role of vibrational energy in promoting gas-surface reactivity^{1,2} is being driven by elegant new laser/molecular beam techniques that can measure vibrational eigenstate-resolved dissociative sticking probabilities³⁻⁵ for molecules impinging on surfaces. Supersonic molecular beam studies of the activated dissociation of H₂ on Cu^{6,7} and CH₄ on W (Refs. 8 and 9), Ni (Refs. 10 and 11), Pt (Ref. 12), and Ru (Ref. 13) surfaces provided early demonstrations that vibrational energy promotes reactivity when vibrational populations are moved, less surgically than with a laser, using heated molecular beam nozzles. Semi-empirical analysis¹⁴ of experiments to date has typically indicated that vibrational energy is similar to, or not quite as effective as, translational energy in promoting activated dissociative chemisorption. Under the assumption that only the ν_3 antisymmetric C-H stretching vibrational mode is active in methane dissociative chemisorption, extrapolations of methane molecular beam experiments to the thermal equilibrium conditions of catalysis, led to predictions that methane vibrationally excited to $\nu_3 = 1$ dominates the thermal dissociative sticking on Ni(100)¹¹ while the ground state dominates on Ru(001).¹³ Later study of the eigenstate-resolved dissociative sticking of CH₄ ($1 \nu_3$, $J = 2$) on Ni(100) (Ref. 3) established that vibrationally excited modes other than

just ν_3 must substantially contribute to the activated sticking observed in conventional molecular beam¹¹ and thermal catalysis¹⁵ experiments. Very recently, vibrational mode-specific dissociative chemisorption was reported for CD₂H₂ on Ni(100) where the dissociation probability was observed to vary by as much as a factor of 5 when molecules were prepared in two different rovibrational eigenstates with virtually identical energies.¹⁶

Dissociative chemisorption of methane on Ni(100) has been subjected to particularly intense experimental and theoretical scrutiny because of its relevance to the large-scale industrial process of steam reforming of natural gas over supported Ni catalysts.¹⁷ Several theoretical studies on reduced dimensionality potential energy surfaces have suggested that CH₄/Ni(100) dissociative chemisorption should be mode specific—displaying a dynamical propensity to react from favored vibrational^{18,19} or rotational²⁰ quantum states. Arguing against such mode specificity, a three-parameter, full dimensionality, physisorbed complex (PC) microcanonical unimolecular rate theory (MURT) applied to CH₄ and CD₄ on Ni(100) (Ref. 21) was able to *quantitatively* predict the dissociative sticking of all the most recent eigenstate-resolved^{3,5} and heated-nozzle¹¹ molecular beam experiments, as well as millibar pressure thermal equilibrium “bulb” experiments.¹⁵ This set of roughly 100 nonequilibrium and equilibrium dissociative sticking experiments spanning eight-orders of magnitude in sticking probability, ten

^{a)}Fax: (434) 924-3710. Electronic mail: harrison@virginia.edu

orders of magnitude in pressure, and a wide experimental parameter space (e.g., rovibrational eigenstates, isotopes CH_4 and CD_4 , E_i , T_n , T_s) could all be predicted by the three-parameter PC-MURT with an average relative discrepancy of 43%. Although methane dissociative chemisorption has at various times been proposed to be dominated by tunneling,^{8,22,23} or by translational or vibrational energy induced molecular deformations (i.e., splat mechanism),^{10,24} the PC-MURT is a conventional transition state theory that assumes CH_4 dissociative chemisorption occurs by over-the-barrier passage of a transition state located along a C-H stretching reaction coordinate. In this paper, we employ the PC-MURT to explore the role of vibrational energy in the dissociative chemisorption of methane on Ni(100).

A. Applicability of a statistical treatment of gas-surface reactivity

A recurrent question has been whether or not a statistical theory with a few dynamical constraints, such as the PC-MURT, can capture the essential chemical physics of methane dissociative chemisorption or is a fully dynamical treatment required.^{2,16,25–28} Much of our most detailed knowledge of gas-surface interactions derives from scattering rare gases and diatomic molecules off surfaces at relatively low energies²⁹—a domain in which low-dimensional dynamical theories often excel. Statistical theories are more appropriate to systems with many degrees of freedom, high state density, and sufficient mode coupling between the various degrees of freedom to support rapid exchange of energy. It is precisely at reactive energies, where a system becomes capable of accessing the distorted transition state region of its potential energy surface (PES), that mode couplings between different degrees of freedom should dramatically strengthen and thereby increase state mixing and rates of intramolecular vibrational energy redistribution (IVR). A measure of the distortion of the PES at the transition state for the $\text{CH}_4/\text{Ni}(100)$ system is that the reaction threshold energy for C-H bond scission drops to $E_0 = 65$ kJ/mol at the Ni surface,²¹ down from 432 kJ/mol for methane in the gas phase. Generally, either at surfaces or in homogeneous phases, state densities in polyatomic molecules are too high at energies sufficient to rearrange *covalent* bonds for spectroscopic assignment of individual quantum states—the spectra are simply too congested and appear chaotic because of strong mode coupling and the high degree of state mixing of the zeroth-order normal mode vibrational states.³⁰ Indeed, for the extensive mixing characteristic of *reactive* energies each molecular eigenstate becomes essentially a microcanonical mixture of the zeroth-order normal mode states.³¹ In the gas phase, IVR is observed in polyatomic molecules at energies where vibrational state densities exceed ~ 10 – 100 states/cm⁻¹. The PC-MURT assumes that dissociative chemisorption occurs competitively with desorption from a localized gas-surface collision complex formed in the vicinity of the physisorption potential well. Vibrational state densities for these transient “physisorbed complexes” consisting of an incident molecule interacting with several surface atoms (oscillators) are greater than 10^5 states/cm⁻¹ even at the threshold energy for dissociative chemisorption. At reactive energies, the phys-

isorbed complex state density is well above the typical onset for IVR (i.e., ≥ 10 – 100 state/cm⁻¹) and access to the distorted transition state region of the PES may lead to very strong mode coupling and ultrafast IVR. As a microcanonical theory, the PC-MURT assumes that all PC states at an energy E become equally probable and react with a common dissociative sticking coefficient, $S(E)$, independent of how the system is initially prepared (e.g., using incident gas-phase molecules in a single rovibrational eigenstate). According to Rice-Ramsperger-Kassel-Marcus (RRKM) theory the desorption-limited lifetime of a PC in the ~ 20 kJ/mol $\text{CH}_4/\text{Ni}(100)$ physisorption well is several picoseconds at the reactive energies of interest (i.e., $E > E_0 = 65$ kJ/mol). The success of the PC-MURT in modeling experiments suggests that a microcanonical distribution is being experimentally approximated over the lifetime of the transient PC, presumably by virtue of rapid, ensemble averaged, randomization of energy through the collisional excitation process on a PES that promotes state mixing²⁵ and supports ultrafast IVR at reactive energies.²⁸

Persistent collision complexes have been observed in crossed molecular beam studies of gas-phase reactions in which a potential well exists along the reaction path between reactants and products (e.g., $A + BC \xrightleftharpoons[k_r]{k_d} ABC \longrightarrow AB + C$).^{32–34} For long-lived collision complexes whose lifetime exceeds a rotational period the measured reactive angular and translational energy distributions are generally found to be consistent with linear and angular momentum conserving, microcanonical theories that postulate that the available collision energy becomes randomized over the internal degrees of freedom of the complex. For example, the barrierless reaction $\text{Nb} + \text{C}_2\text{H}_4 \rightarrow \text{NbC}_2\text{H}_2 + \text{H}_2$ was recently shown to proceed through a long-lived intermediate (bound by 150 kJ/mol) by virtue of its statistical reactive and nonreactive angular and translational energy distributions that were measured over a wide range of center-of-mass collision energies from 20 to 97 kJ/mol.³⁵ Clearly, considerable center-of-mass collision energy can be transiently converted into internal degrees of freedom of the collision complex and statistically mixed over the complex lifetime of at least a rotational period of several picoseconds. The lifetime of the persistent collision complex of the $\text{Br} + \text{I}_2$ reaction has been directly measured by femtosecond studies of photoinitiated reactions of $\text{HBr} \cdots \text{I}_2$ van de Waals precursors³⁶ and indirectly determined by microcanonical theoretical analysis of crossed molecular beam experiments.³⁷ The lifetime of the BrII complex (bound by ~ 60 kJ/mol) was $\tau \sim 44$ ps at a center-of-mass collision energy of 1.7 kJ/mol, dropping to $\tau \sim 5$ ps and 3 ps for collision energies of 52 kJ/mol and 87 kJ/mol, respectively. Collision complex lifetimes decrease with increasing energy and may eventually become too short for IVR to provide complete statistical mixing of the energy. This limiting scenario is apparently achieved in the surface induced dissociation of some polyatomic ions at incident ion beam energies of ~ 3000 kJ/mol.^{38,39} The much lower collision energies relevant to dissociative chemisorption of CH_4 on Ni(100) are comparable to those of the gas-phase reactions discussed above which form persistent collision com-

plexes that react statistically. The PC-MURT model should be applicable if, at reactive energies, IVR completes on the time scale of the several picoseconds that the $\text{CH}_4/\text{Ni}(100)$ PCs are calculated to persist.

Although direct and completely unambiguous experimental evidence for ultrafast IVR in gas-surface collision complexes formed at chemically significant energies is currently lacking, an interesting example of ultrafast energy transfer is provided by the surprisingly efficient vibrationally inelastic scattering of $\text{H}_2(v=0)$ from $\text{Cu}^{40,41}$ at reactive energies where access to the state-mixing transition state region of the potential energy surface is possible.⁴² For the H_2/Cu scattering system, the large energy mismatch between the quanta of the relatively stiff molecular vibrations and those of the softer surface phonons (i.e., $\nu_{\text{H}_2}=4159\text{ cm}^{-1}$ and the Debye phonon energy is 238 cm^{-1} for Cu) should make vibrational energy transfer difficult according to the usual exponential energy gap laws based on weak anharmonic mode coupling.⁴³ The point worth making is that our intuition about gas-surface collisions, even for those systems that do behave dynamically at low energies where state densities and mode couplings are modest, may fail us at reactive energies where state densities and mode couplings can be high.

Dissociative sticking experiments are typically ensemble averaged over many gas-surface collisions without control over the molecular orientation, phase of vibration, or collisional impact position across a surface unit cell. It has sometimes been argued that similar collisional averaging in gas-phase unimolecular reactions might generate an ensemble averaged random distribution of vibrational energy in the reacting species that would suffice for experimental mimicry of microcanonical RRKM kinetics without any requirement for additional IVR.^{44,45} For collisionless gas-phase unimolecular dissociation prompted by lasers, even for small molecules such as NO_2 (Ref. 46) and D_2CO , (Ref. 47) detailed adherence to RRKM kinetics is generally found and in the absence of collisions this must be based on rapid IVR at reactive energies.³⁰ Although rare, non-RRKM unimolecular decomposition kinetics on an electronic ground state PES can be observed in gas-phase polyatomic systems where IVR is sufficiently slow (e.g., $\text{HCO}_{(g)}$).⁴⁸ Similarly, the mode-specific dissociation of CD_2H_2 on $\text{Ni}(100)^{16}$ may occur because insufficient mode coupling within the PCs leads to slow IVR in comparison to desorption which competes with dissociation at the surface.

The success of the PC-MURT in modeling CH_4/CD_4 dissociative chemisorption cannot be taken as incontrovertible proof for ultrafast IVR in the PCs because the gas-surface collisions themselves provide another avenue for energy randomization. The relative importance of these two mechanisms by which an ensemble averaged microcanonical vibrational energy distribution in the transient PCs might be attained is currently unknown. As discussed at greater length elsewhere,²⁸ the 100–500 fs and ~ 10 ps IVR lifetimes at relatively modest vibrational excitation energies for $\text{CH}_{4(g)}$ (Ref. 49) and $\text{CH}_2\text{I}_{2(l)}$, (Ref. 50) respectively, are suggestive that IVR lifetimes for the 15 degrees of freedom $\text{CH}_4/\text{Ni}(100)$ PCs at reactive energies will be shorter than the PC desorption lifetime of $\tau_d \sim 2$ ps. If PC IVR lifetimes

are indeed this short then PC-MURT kinetics should apply even before figuring in the additional energy randomizing and averaging influence of the initial gas-surface collisions.

The vibrational structure of CH_4 and CD_4 naturally make these molecules relatively good candidates for IVR at higher energies because the normal mode stretching frequencies ($\nu_1 \approx \nu_3$) are essentially twice the bend frequencies ($\nu_2 \approx \nu_4$), leading to Fermi resonances and clumping of the zeroth-order normal mode states into polyad energy bands characterized by a single polyad quantum number, $N = 2(\nu_1 + \nu_3) + \nu_2 + \nu_4$.⁵¹ The vibrational eigenstates can be described perturbatively as mixtures of the different normal modes.⁵² The vibrational structure of CD_2H_2 is more complicated because there are nine different normal mode frequencies and its energy level clumpings lead to two different polyad quantum numbers. Consequently, the CD_2H_2 methane isotopomer is not so favorable a candidate for IVR and facile mixing of the normal mode states at higher energies. Reactive evidence that local modes can persist even when two quanta of C-H stretch are excited comes from the vibrational mode-specific gas-phase reaction of Cl atoms with CD_2H_2 to form HCl and CD_2H .⁵³ In this reaction, state resolved experiments indicate that Cl preferentially attacks a vibrationally excited C-H bond and the adjacent CD_2H acts as a spectator species that largely preserves its initial vibrational state. Gas-phase reaction rates for Cl atoms reacting with vibrationally excited CH_4 in the $(\nu_1 + \nu_4)$ state versus the essentially isoenergetic $(\nu_3 + \nu_4)$ state were a factor of 1.9 ± 0.5 higher⁵⁴ suggesting that vibrational mode-specific effects on overall reaction rates may be relatively modest for this direct reaction.⁵⁵ Greater mode specificity was reported for the dissociative chemisorption of vibrationally excited CD_2H_2 on $\text{Ni}(100)^{16}$ where the dissociative sticking probability was as much as five times higher for the $|2\ 0\rangle$ state, with 2 quanta of C-H stretching excited in a single C-H bond, as compared to the isoenergetic $|1\ 1\rangle$ state, with one quantum in each of the two C-H bonds. In this paper, we show by comparison to experiments that the dissociative chemisorption of methane on $\text{Ni}(100)$ can be quantitatively treated using the statistical PC-MURT for some methane isotopomers, CH_4 and CD_4 , but not for CD_2H_2 .

Molecular beam experiments measuring initial dissociative sticking coefficients S are often fit based on the ansatz that molecules with vibrational state ν_i , rotational state J , and translational energy E_t incident on a surface at temperature T_s will dissociatively stick according to an “erf” functional form^{6,7}

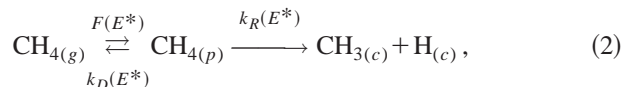
$$S(\nu_i, J, E_t; T_s) = \frac{A(\nu_i, J)}{2} \left[1 + \text{erf} \left(\frac{E_t - E_0(\nu_i, J)}{W(\nu_i, J; T_s)} \right) \right], \quad (1)$$

which has been remarkably successful when applied to H_2 dissociative chemisorption on Cu. There are three free parameters for each (ν_i, J) state: an amplitude, $A(\nu_i, J)$; center point energy, $E_0(\nu_i, J)$; and a width parameter, $W(\nu_i, J; T_s)$. The sticking observed in molecular beam experiments with heated nozzles or in thermal equilibrium bulb experiments is the sum of contributions from all thermally populated (ν_i, J) states and must be averaged over the incident molecular translational energy distribution. Problematic for this mo-

lecular quantum state resolved description of sticking is that (i) in the absence of a rigorous theoretical basis for the Eq. (1) ansatz,¹⁴ it is difficult to ascribe any physical significance to its modeling parameters and (ii) to predict methane dissociative sticking from molecular beam experiments with heated nozzles or thermal equilibrium bulb experiments would require a great many state-of-the-art eigenstate-resolved experiments to define the necessary modeling parameters for each of the thermally populated (ν_i, J) states. In contrast, the PC-MURT does not suffer these problems and requires only three parameters to make quantitative predictions for any conceivable experiment concerning methane dissociative chemisorption on Ni(100). In this paper, we derive expressions for fitting or predicting the dissociative sticking in molecular beam and thermal bulb experiments on the basis of molecular vibrational state resolved sticking coefficients and compare the predictions of the PC-MURT to those made using the Eq. (1) ansatz and other dynamical theories.

II. PC-MURT: THEORETICAL MODEL

We assume the methane dissociative chemisorption kinetics can be described microcanonically as^{28,56}



where the E^* zero of energy occurs with methane at infinite separation from the surface when all species are at 0 K. Methane incident on the surface from the gas phase is assumed to form a transient gas/surface collision complex consisting of a molecule, in the neighborhood of the physisorption potential well minimum, that interacts with a few immediately adjacent surface atoms. These collisionally formed PCs or “local hot spots” are energetic and transient intermediate species that are not in thermal equilibrium with the surrounding substrate. Physisorbed complexes formed at some total energy E^* [i.e., $\text{CH}_{4(p)}$ in Eq. (2) where surface coordination numbers are suppressed] can go on to desorb or react dissociatively with the surface to yield chemisorbed fragments with RRKM rate constants $k_D(E^*)$ and $k_R(E^*)$. Initial dissociative sticking coefficients S are experimentally derived from the ratio of the deposited C coverage, typically measured by Auger electron spectroscopy, to the incident fluence of methane molecules, extrapolated backwards to zero net fluence. The steady state approximation applied to the $\text{CH}_{4(p)}$ coverage of Eq. (2) yields a PC-MURT that predicts

$$S = \int_0^\infty S(E^*) f(E^*) dE^*, \quad (3)$$

where

$$S(E^*) = \frac{W_R^\ddagger(E^* - E_0)}{W_R^\ddagger(E^* - E_0) + W_D^\ddagger(E^*)} \quad (4)$$

is the microcanonical sticking coefficient, W_i^\ddagger is the sum of states for transition state i , E_0 is the apparent threshold energy for dissociation, and

$$f(E^*) = \int_0^{E^*} f_t(E_t) \int_0^{E^* - E_t} f_v(E_v) \int_0^{E^* - E_t - E_v} f_r(E_r) \times f_s(E^* - E_t - E_v - E_r) dE_r dE_v dE_t \quad (5)$$

is the probability distribution for creating a physisorbed complex at E^* . $f(E^*)$ is formed by convolution over the distribution functions for the flux weighted translational energy, vibrational energy, and rotational energy of the incident methane, along with the surface energy distribution for s oscillators vibrating at the mean Ni phonon frequency, $\nu_s = 3/4 k_b T_{\text{Debye}}/h$, of 235 cm^{-1} .

The molecular beam studies of methane dissociative chemisorption on Ni(100) find that the dissociative sticking coefficient scales with the translational energy directed along the surface normal, $E_n = E_t \cos^2 \vartheta$. Discounting parallel molecular translational energy as a spectator or inactive form of energy over the course of the reactive gas-surface collisions, we assume that only normal translation will contribute to E_t in the expressions above (i.e., set $E_t = E_n$ alone). Following common practice, we further assume that the molecular beam nozzle temperature T_n sets the vibrational and rotational temperatures of the beam molecules as $T_v = T_n$ and $T_r = 0.1 T_n$, respectively.

Once the transition state characteristics have been defined through iterative simulation of varied experimental data or by electronic structure theory calculations, any experimental sticking coefficient can be predicted using Eq. (3) to average the microcanonical sticking coefficient over the probability for creating a physisorbed complex at E^* under the specific experimental conditions of interest. Given that $S(E^*)$ is simply the ratio of the available exit channels through the reactive transition state to the total number of exit channels available through either the reactive or desorptive transition states [Eq. (4)], the PC-MURT provides a statistical description of the chemisorption kinetics.

In the absence of definitive guidance from electronic structure calculations, and in the spirit of employing a surface kinetics theory with a minimum number of adjustable parameters, we assume the transition states for desorption and dissociation are loose and share as many common mode frequencies with each other as possible. The transition state for desorption is taken to occur when methane is freely rotating and vibrating in the gas phase, far from the surface. The dissociation transition state is characterized by the nine vibrational modes of methane in the gas, s vibrational modes of the surface oscillators, four vibrational modes at a single lumped frequency ν_D representative of the three frustrated rotations and the vibration along the surface normal of methane at the dissociation transition state, and one of the triply degenerate antisymmetric C-H stretching vibrations [$\nu_3(\text{CH}_4) = 3020 \text{ cm}^{-1}$] of methane is sacrificed as the reaction coordinate. The resulting PC-MURT has only three adjustable parameters, E_0 , ν_D , and s , that can be fixed by comparison of simulations to varied experimental data. An optimal parameter set of ($E_0 = 65 \text{ kJ/mol}$, $\nu_D = 170 \text{ cm}^{-1}$, $s = 2$) was recently found²¹ by simulating the eigenstate resolved molecular beam data of Schmid *et al.*⁵ As shown in Fig. 1, this parameter set successfully predicts the results of

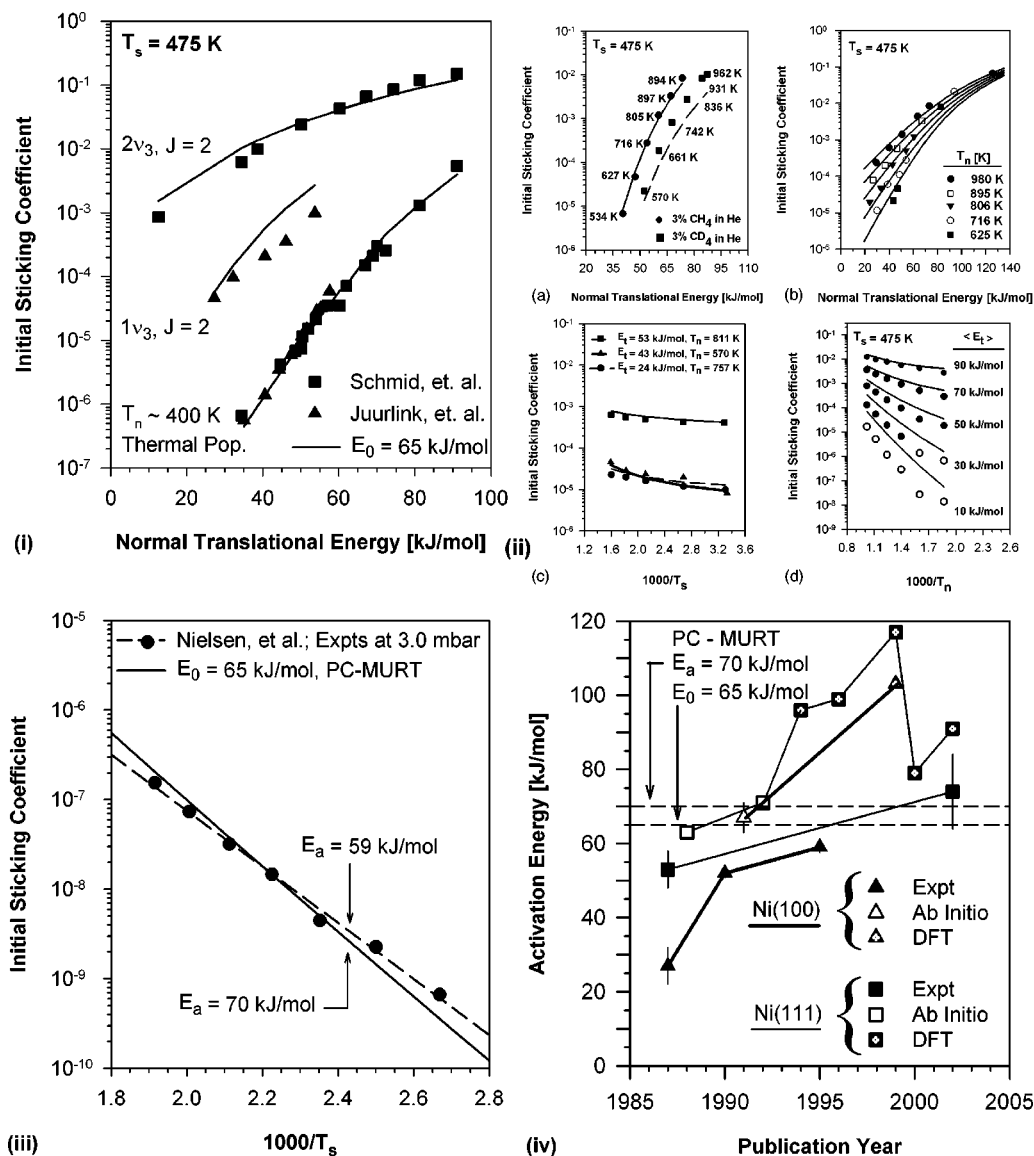


FIG. 1. (i)–(iii) Comparison of the most recent experimentally derived initial dissociative sticking coefficients (points) for CH₄ impinging on Ni(100) with the theoretical predictions of the PC-MURT (lines) based on $E_0 = 65$ kJ/mol, $\nu_D = 170$ cm⁻¹, and $s = 2$. (i) Molecular beam experiments for $T_n \sim 400$ K and for single vibrationally excited eigenstates ($1\nu_3, J=2$)³ and ($2\nu_3, J=2$).⁵ The Juurlink *et al.* sticking coefficients have been divided by 5.9. (ii) Molecular beam derived sticking coefficients of Holmblad *et al.*¹¹ have been divided by 4.5. T_n values have been recalculated⁵⁶ according to calibration experiments¹⁷ and in frame (a) are given beside each experimental sticking point. (iii) Thermal equilibrium bulb experiments¹⁵ at 3 mbar pressure. (iv) Activation energies for CH₄ dissociative chemisorption, E_a , derived experimentally^{15,60,71,72} and apparent threshold energies, E_0 ($= E_a$ at 0 K), derived from *ab initio*^{57,73,74} or density functional theory^{75–79} electronic structure calculations are compared to the predictions of the PC-MURT.

the other recent molecular beam and thermal equilibrium bulb experiments and the apparent threshold energy of $E_0 = 65$ kJ/mol is consistent with the 67 ± 4 kJ/mol value calculated by *ab initio* electronic structure theory.⁵⁷ The $E_0 = 65$ kJ/mol parameter set will be used in all further PC-MURT calculations below.

Rescaling of the experimental data of Juurlink *et al.*³ and Holmblad *et al.*¹¹ in Fig. 1(i) and 1(ii) was optimized²¹ for best agreement with the predictions of the PC-MURT. Currently, this experimental rescaling seems appropriate. Order of magnitude differences in dissociative sticking coefficients as a function of E_t [i.e., $S(E_t; T_n, T_s)$] reported by different molecular beam laboratories are not uncommon,¹⁷ although almost invariably there are differences in the T_n and T_s experimental conditions that makes direct comparisons difficult

to assess in the absence of a well agreed upon theoretical model that can predict the results of such nonequilibrium experiments. Although experimental reproducibility from a particular laboratory may be excellent, precise calibration of absolute sticking coefficients is undoubtedly very difficult to achieve, especially when sticking coefficients are small (e.g., $S < 10^{-3}$). Consequently, the introduction of scaling factors to renormalize sticking coefficients derived from some laboratories, in an effort to recover a common “absolute” sticking scale is not unreasonable. In Figure 1(i) essentially identical experimental measurements of $S(E_t; T_n \sim 400$ K, $T_s = 475$ K) versus E_t were made by Schmid *et al.*⁵ with 373 K $< T_n < 473$ K and $\langle T_n \rangle = 409$ K and also by Juurlink *et al.* with $T_n = 400$ K. Division of the sticking coefficients, published by Juurlink *et al.* by a factor of 5.9 can be seen to

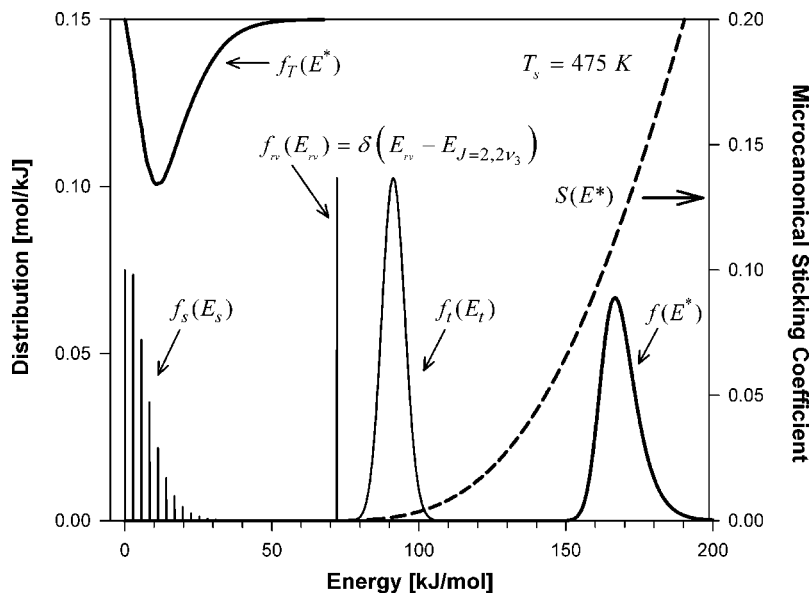


FIG. 2. Surface, rovibrational, and translational energy distributions are shown along with the convolved total energy distribution, $f(E^*)$, for the highest energy ($2\nu_3, J=2$) molecular beam experiment of Fig. 1(i) at $T_s=475$ K. The thermal energy distribution, $f_T(E^*)$, appropriate to a high pressure bulb experiment of Fig. 1(iii) at $T=475$ K is shown for comparison and has been inverted for clarity. The microcanonical sticking coefficient, $S(E^*)$, is also depicted. Averaging $S(E^*)$ over these $f(E^*)$ s with the same T_s according to Eq. (3) yields the experimental sticking coefficients, 0.15 and 4×10^{-8} , respectively.

lead to good agreement between the $S(E_t; T_n \sim 400$ K, $T_s = 475$ K) values derived from both experimental laboratories and with the predictions of the PC-MURT. Discussions amongst the leaders of the different molecular beam laboratories investigating dissociative chemisorption of CH_4 on Ni(100) suggest that the sticking coefficients reported by Juurlink *et al.* and Homblad *et al.* should be reduced by factors near 5 based on recent experimental and cross-laboratory calibrations.⁵⁸

Figure 2 provides a comparison of the physisorbed complex energy distributions for the highest energy [$\langle E_t \rangle = 91$ kJ/mol, ($2\nu_3, J=2$) eigenstate, $T_s=475$ K] molecular beam experiment of Fig. 1(i) and the thermal equilibrium bulb experiment of Fig. 1(iii) at the same surface temperature. The $\langle E^* \rangle = 169$ kJ/mol mean energy of the beam experiment compares to $\langle E^* \rangle = 17$ kJ/mol for the bulb experiment that was performed at ten orders of magnitude higher pressure. Averaging the microcanonical sticking coefficient over the energy distributions of these experiments according to Eq. (3) yields experimental sticking coefficients that differ by eight orders of magnitude. Although the high energy ($2\nu_3, J=2$) single eigenstate beam experiment is very far from thermal equilibrium (i.e., $T=T_s=475$ K) in both its translational and internal energy distributions, the PC-MURT, which assumes that energy becomes microcanonically redistributed within the transiently formed physisorbed complexes, performs well. Defining the average relative discrepancy (ARD) between the PC-MURT predictions and experiment as

$$\text{ARD} = \left\langle \frac{|S_{\text{theory}} - S_{\text{expt}}|}{\min(S_{\text{theory}}, S_{\text{expt}})} \right\rangle,$$

the ARD for both the Fig. 1(i) Schmid *et al.*⁵ and Fig. 1(iii) Nielsen *et al.*¹⁵ data sets is 33%. The ARD for the rescaled Juurlink *et al.*³ data of Fig. 1(i) and Homblad *et al.*¹¹ data of Fig. 1(ii) is 64% and 43%, respectively. The overall ARD for the 96 varied nonequilibrium and equilibrium experiments of Fig. 1 is 43%.

The success of the PC-MURT in describing the ($2\nu_3, J=2$) eigenstate resolved sticking is noteworthy because methane's highest frequency vibrational mode ν_3 should be the most difficult one to relax through energy exchange with lower frequency physisorbed complex vibrational modes or surface phonons according to conventional exponential energy gap laws. However, as can be seen in Fig. 3, at reactive energies the physisorbed complex density of states is high ($>10^5$ state/cm⁻¹) and there is always a large bath of isoenergetic states of different mode character with which to undergo rapid IVR. Consequently, an energy gap between the normal mode fundamentals is not the key issue restraining IVR, it is only the degree of mode coupling at these reactive energies. The success of the PC-MURT ap-

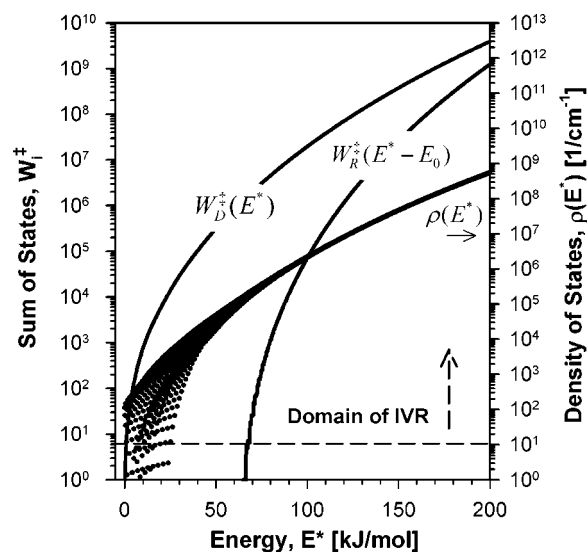


FIG. 3. The sum of states for the desorption and reaction transition states are shown along with the density of states for the physisorbed complex. At reactive energies, $E^* \geq 65$ kJ/mol, the physisorbed complex density of states is $\geq 10^5$ states/cm⁻¹, well above the typical 10 states/cm⁻¹ onset for intramolecular vibrational energy redistribution (IVR) in gas-phase molecules.

plied to CH_4 and CD_4 in Fig. 1 argues for strong mode coupling and ultrafast IVR (i.e., faster than $\tau_d \sim 2$ ps).

Although Juurlink *et al.*³⁴ and Schmid *et al.*⁵ have specifically argued that their CH_4 eigenstate-resolved molecular beam results rule out a statistical model for CH_4 dissociation on Ni(100), Fig. 1 demonstrates that the PC-MURT is entirely compatible with their experiments. These exclusionary claims were based on the notion that values of a semi-empirically defined “translational efficacy,” [e.g., $\beta_t = \partial(\ln S)/\partial(E_t)$], and “vibrational efficacy” [e.g., $\beta_v = \partial(\ln S)/\partial(E_v)$] should be numerically identical if a statistical theory applies. However, as analytically derived elsewhere in the context of the PC-MURT,²⁸ β_t and β_v are functions of the experimental specifics and are not generally especially diagnostic of whether a statistical or dynamical theory applies. A statistical theory only requires $\beta_i|_{E^*} = \beta_v|_{E^*}$ where both efficacies are evaluated precisely when the physisorbed complexes being formed have the same total energy (i.e., $E^* = E_t + E_v + E_r + E_s$). Arranging such a comparative scenario using molecular beams has not been specifically pursued in the past, and at best may only be approximated in an averaged sense because the molecular and surface distribution functions over the various kinds of energy can not all be simultaneously prepared as δ functions (see Fig. 2).

A ($2\nu_3, J=2$) eigenstate-resolved molecular beam dissociative sticking measurement at a single translational energy for CH_4 on Pt(111) at Princeton has also been cited as evidence that a statistical model of gas-surface reactivity is inadequate.⁴ The dissociative sticking coefficient for CH_4 impinging on Pt(111) in the ($2\nu_3, J=2$) eigenstate at $E_t = 5$ kJ/mol was $S = 1.8 \times 10^{-4}$, a relatively modest 30-fold enhancement over a $T_n = 295$ K beam at the same energy. In contrast, sticking of the CH_4 ($2\nu_3, J=2$) eigenstate on Ni(100) at $E_t = 12$ kJ/mol was $S = 5 \times 10^{-4}$, believed to be a more than 10^4 -fold enhancement over a $T_n = 400$ K beam at the same energy⁵ [see Fig. 1(i)]. The Princeton group pioneered two new and unusual techniques to make their measurements: helium beam scattering to measure surface carbon deposited by methane and the use of a cw laser build-up cavity for overtone pumping of the methane beam. Their conclusion that a statistical model is inadequate is surprising because the PC-MURT has previously been used quite successfully to model dissociative sticking of methane on Pt(111)^{25,28} over a wide range of experimental conditions measured using two separate molecular beam machines^{12,23} at IBM.

Nevertheless, as shown in Fig. 4, the PC-MURT certainly cannot predict the vibrational mode-specific dissociative sticking reported for CD_2H_2 on Ni(100).¹⁶ The PC-MURT calculations for CD_2H_2 assumed that dissociation could occur by breaking either a C-H or C-D bond and that all molecular orientations with respect to the surface are equally probable. The PC-MURT predicts that the dissociative sticking for a $T_n = 423$ K molecular beam should be reduced about 11-fold on going from CH_4 to CD_2H_2 . This reduction in sticking stems primarily from the increase in available desorption states open to CD_2H_2 because of its smaller rotational constants and smaller symmetry number

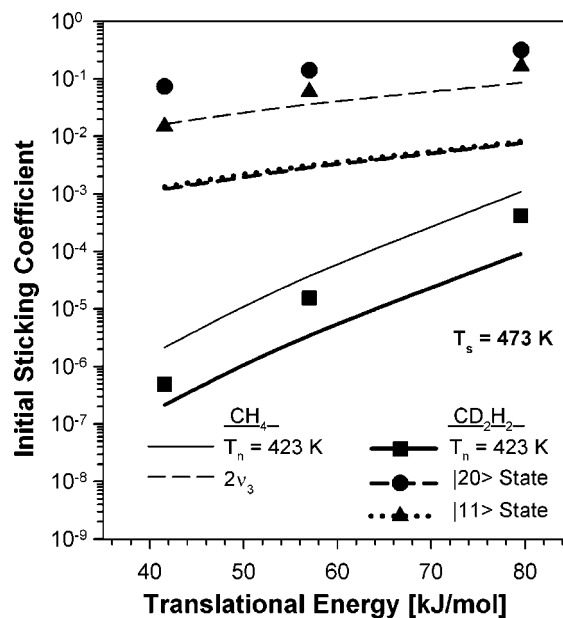


FIG. 4. Comparison of experimental (points) and PC-MURT (heavy lines) derived initial dissociative sticking coefficients for CD_2H_2 incident on Ni(100). The CD_2H_2 sticking is shown for a thermally populated molecular beam with $T_n = 423$ K and for different rovibrational eigenstates with two quanta of C-H stretching excited: $|1\ 1\rangle = (1\nu_1, 1\nu_6; J=1)$ and $|2\ 0\rangle = (2\nu_1; J=1)$. Thin lines give PC-MURT predictions for comparable sticking experiments for CH_4 incident on Ni(100).

(e.g., $\sigma=2$, down from 12), and secondarily from the kinetic isotope effect. Experimentally, the thermal beam sticking falls only about threefold on going from CH_4 to CD_2H_2 . The PC-MURT underestimates the CD_2H_2 dissociative sticking for the $T_n = 423$ K beam, $|1\ 1\rangle$ state (6000.2 cm^{-1}), and the $|2\ 0\rangle$ state (5879.8 cm^{-1}) by factors of about 4, 20, and 50, respectively. Surprisingly, in light of the kinetic isotope effect, the CH_4 dissociative sticking for the $2\nu_3$ state (6004.69 cm^{-1}) is less than that for either of the two CD_2H_2 states at comparable levels of vibrational excitation. As discussed above, the failure of the PC-MURT to accurately predict the CD_2H_2 sticking might be caused by overly slow IVR within the PCs formed involving this molecule.

Given that the PC-MURT appears to accurately predict the dissociative sticking for CH_4 and CD_4 on Ni(100), but not for CD_2H_2 , we will pragmatically restrict our calculations and analysis below to just the $\text{CH}_4/\text{Ni}(100)$ system. The results should be broadly illustrative of the kinetics for any gas-surface dissociative chemisorption system that behaves statistically.

III. VIBRATIONAL STATE RESOLVED DISSOCIATIVE STICKING FROM MOLECULAR BEAMS

According to Eqs. (3)–(5), the dissociative sticking coefficient can be calculated as

$$S = \int_0^\infty S(E^*) f_{vtrs}(E^*) dE^*,$$

$$S = \int_0^\infty S(E^*) \left\{ \int_0^{E^*} f_v(E_v) \left\{ \int_0^{E^*-E_v} f_t(E_t) \right. \right. \\ \left. \left. \times \int_0^{E^*-E_v-E_t} f_r(E_r) \right. \right. \\ \left. \left. \times f_s(E^*-E_v-E_t-E_r) dE_r \right\} dE_t \right\} dE_v \left. \right\} dE^*. \quad (6)$$

If the vibrational and translational energy distributions of the molecules incident on the surface in an idealized molecular beam experiment are δ functions, $f_v(E_v) = \delta(E_v - E'_v)$ and $f_t(E_t) = \delta(E_t - E'_t)$, then only the integration of Eq. (6) over dE^* with $E^* > E'_v + E'_t$ contributes to the sticking after integrations over dE_v and dE_t pick up the δ functions. Consequently,

$$S = \int_{E'_v+E'_t}^\infty S(E^*) \left\{ \int_0^{E^*-E'_v-E'_t} f_r(E_r) \right. \\ \left. \times f_s(E^*-E'_v-E'_t-E_r) dE_r \right\} dE^*. \quad (7)$$

Noting that $E^* = E'_v + E'_t + E_{rs}$ where $E_{rs} = E_r + E_s$ and $dE^* = dE_{rs}$,

$$S = \int_{E'_v+E'_t}^\infty S(E^*) \left\{ \int_0^{E_{rs}} f_r(E_r) f_s(E_{rs}-E_r) dE_r \right\} dE^*, \\ S = \int_0^\infty S(E'_v + E'_t + E_{rs}) f_{rs}(E_{rs}) dE_{rs}. \quad (8)$$

The sticking is an average of the microcanonical sticking coefficient $S(E^*)$ over the probability of forming a PC with energy E^* given specific values of E_v and E_t . This is calculated by an appropriate averaging of $S(E^*)$ over the convolved rotational and surface energy distributions of the particular experiment of interest.

Let us now introduce a simpler, less formal style for manipulating and thinking about these sticking equations and again calculate the sticking for a hypothetical molecular beam experiment with δ function distributions in E_v and E_t , and with rotational and surface distributions characterized by temperatures $T_r = 0.1T_n$ and T_s ,

$$S_v(E_t; T_n, T_s) = \langle S(E_v, E_t) \rangle_{rs} \\ = \int_0^\infty S(E^*) f(E^*; E_v, E_t) dE^*,$$

$$S_v(E_t) = \int_0^\infty S(E^* = E_v + E_t + E_r + E_s) \\ \times \left\{ \int_0^{E^*-E_v-E_t} f_r(E_r) \right. \\ \left. \times f_s(E^*-E_v-E_t-E_r) dE_r \right\} dE^*, \quad (9)$$

$$S_v(E_t) = \int_0^\infty S(E^*) f_{rs}(E^* - E_v - E_t) dE^*,$$

$$S_v(E_t) = \int_0^\infty S(E_v + E_t + E_{rs}) f_{rs}(E_{rs}) dE_{rs}.$$

To make contact with conventional molecular beam sticking measurements, one must average over the flux weighted translational energy distribution,

$$S_v = \langle S_v(E_t) \rangle_t = \int_0^\infty S_v(E_t) f_t(E_t) dE_t, \quad (10)$$

$$S_v = \int_0^\infty \left\{ \int_0^\infty S(E_v + E_t + E_{rs}) f_{rs}(E_{rs}) dE_{rs} \right\} f_t(E_t) dE_t,$$

to yield the vibrational energy resolved sticking coefficient S_v and then average over the thermal vibrational energy distribution,

$$S = \langle S_v \rangle_v = \int_0^\infty S_v f_v(E_v) dE_v = \sum_{E_v} f_v(E_v) S_v, \\ S = \sum_{E_v} f_v(E_v) \left\{ \int_0^\infty S_v(E_t) f_t(E_t) dE_t \right\}, \quad (11)$$

where the beam vibrational temperature is typically given by the nozzle temperature, $T_v = T_n$. As usual, because the vibrational states are discrete,

$$\int_0^\infty f_v(E_v) dE_v = \sum_{\text{Energy levels } E_v} f_v(E_v) = \sum_{\substack{\text{States } v_i \\ \text{e.g., (0202)}}} P_{v_i} = 1, \quad (12)$$

one can keep track of them in several ways. It is convenient to label the CH₄ vibrational states, v_i , by the vibrational quanta in the normal modes (v_1, v_2, v_3, v_4). The probability for an incident molecule with vibrational temperature T_v to strike the surface in vibrational state v_i is

$$P_{v_i} = \frac{g_{v_i}}{Q_v} \exp\left(\frac{-E_{v_i}}{k_b T_v}\right), \quad (13)$$

where g_{v_i} and E_{v_i} are the vibrational state's degeneracy and energy, and Q_v is the vibrational partition function. Recognizing that the PC-MURT is not vibrational mode selective, Eq. (11) can be rewritten as

$$S = \sum_{v_i} P_{v_i} \left\{ \int_0^\infty S_{v_i}(E_t) f_t(E_t) dE_t \right\} \\ = \sum_{v_i} P_{v_i} S_{v_i} = \sum_{v_i} \delta S_{v_i}, \quad (14)$$

where the sums are over vibrational states,

$$S_{v_i}(E_t) = \langle S(E_{v_i}, E_t) \rangle_{rs} = \int_0^\infty S(E_{v_i} + E_t \\ + E_{rs}) f_{rs}(E_{rs}) dE_{rs}, \quad (15)$$

S_{v_i} is a vibrational state resolved sticking coefficient, and δS_{v_i} is the vibrationally resolved contribution to the overall sticking from state v_i under the particular experimental conditions of interest.

Figure 5 shows how the CH₄/Ni(100) dissociative sticking for the thermally populated molecular beam experiments of Fig. 1(i) can be decomposed into contributions from different CH₄ vibrational states. The first 15 vibrationally re-

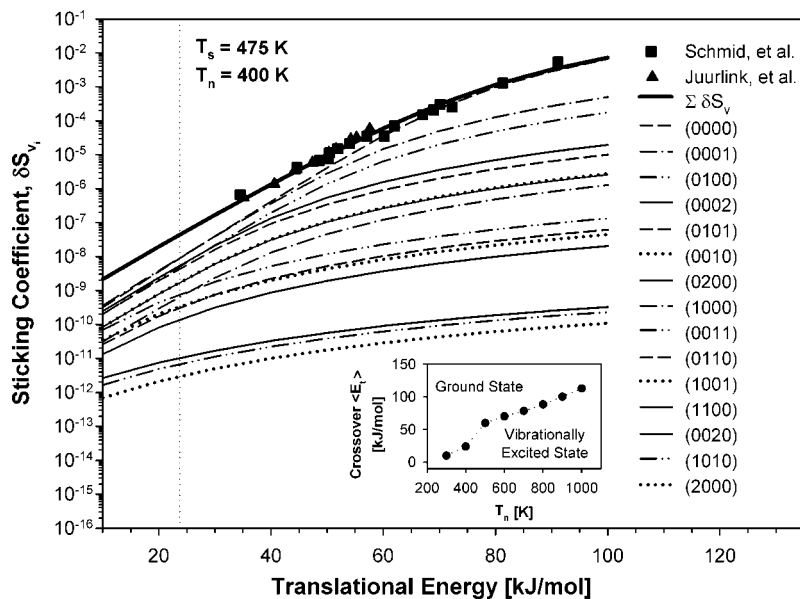


FIG. 5. PC-MURT predictions of vibrationally resolved sticking contributions, δS_{v_i} , relevant to the thermal molecular beam experiments of Fig. 1(i) with $T_n=400$ K and $T_s=475$ K. In these beam experiments, sticking from methane in the $(v_1, v_2, v_3, v_4) = (0000)$ vibrational ground state dominates the sticking for $\langle E_t \rangle \geq 24$ kJ/mol.

solved sticking contributions δS_{v_i} are shown as a function of the mean translational energy of the incident methane. Closed symbols represent molecular beam data taken by Schmid *et al.*⁵ and Juurlink *et al.*³ while the lines give predictions of the PC-MURT. Summing over δS_{v_i} vibrationally resolved sticking contributions recovers the experimental sticking shown in Fig. 1(i) and Fig. 5. The inset graph within Fig. 5 shows the boundary between vibrational ground and excited state dominance in the CH_4 dissociative sticking as a function of both mean translational energy and nozzle temperature. As illustrated by this inset, the crossover $\langle E_t \rangle$, or mean translational energy at which the ground state becomes the predominant mode governing the dissociative sticking, increases as the beam nozzle temperature increases. For the 400 K nozzle temperature of the Fig. 1(i) molecular beam experiments the predicted crossover energy is 24 kJ/mol, an energy which is marked as the dotted vertical line in Fig. 5. For incident mean translational energies below 24 kJ/mol, the sticking is dominated by vibrational states with excited bending modes.

Figure 6 depicts the fractional sticking contributions of the five vibrational states most important to the overall sticking of Fig. 5, along with the sum of their fractional contributions as a function of translational energy. The ground vibrational state generally contributes most to the dissociative sticking. However, at translational energies below 24 kJ/mol, vibrationally excited states of the ν_4 bending mode become particularly important contributors to the overall sticking because of the especially low energy and high degeneracy of these states (e.g., $E_{(0001)} = 1305 \text{ cm}^{-1}$, $g_{(0001)} = 3$).

Vibrationally resolved sticking curves $S_{v_i}(E_t)$ calculated using Eq. (15) are depicted in Fig. 7 for the first 15 vibrationally excited states of methane. These vibrational states are energy bunched into five polyad bands with polyad quantum number, $N = 2(\nu_1 + \nu_3) + \nu_2 + \nu_4$, ranging from 0 to 4. Given the narrow energy bandwidth of each polyad, the $S_{v_i}(E_t)$ curves for vibrational states within each polyad are very similar. The $S_{v_i}(E_t)$ curves are S shaped and approach 1

in the limit of sufficiently high E_t . As shown in Eq. (14), averaging a $S_{v_i}(E_t)$ curve over the flux weighted translational energy distribution of the molecular beam and weighting the result by the Boltzmann probability of finding the ν_i vibrational state in the beam yields the vibrationally resolved dissociative sticking contribution δS_{v_i} of the kind plotted in Fig. 5.

Holmblad *et al.*¹¹ employed Eq. (14) with a rotationally averaged form of Eq. (1),

$$S_{v_i}(E_t) = \frac{A_{v_i}}{2} \left[1 + \text{erf} \left(\frac{E_t - E_{0,v_i}}{W_{v_i}(T_s)} \right) \right], \quad (16)$$

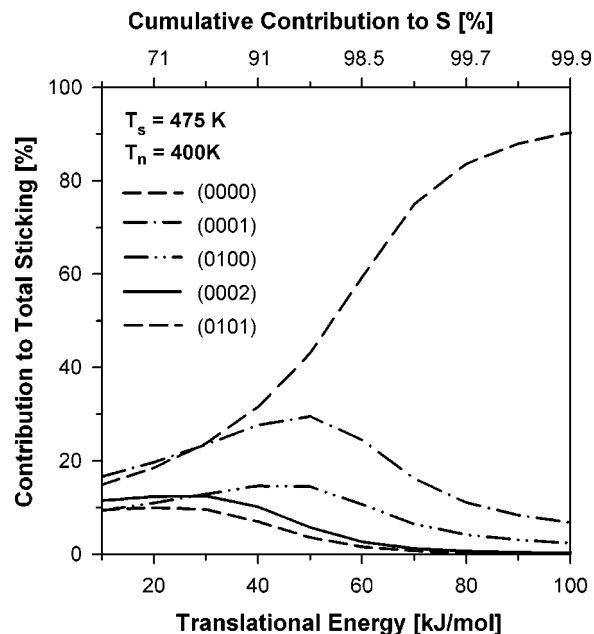


FIG. 6. PC-MURT predictions of the most important vibrationally resolved sticking contributions relevant to the thermal molecular beam experiments of Fig. 1(i), displayed as fractions of the overall sticking. Cumulative contributions to the overall sticking derived by vertically summing the δS_{v_i} are given on the upper x axis.

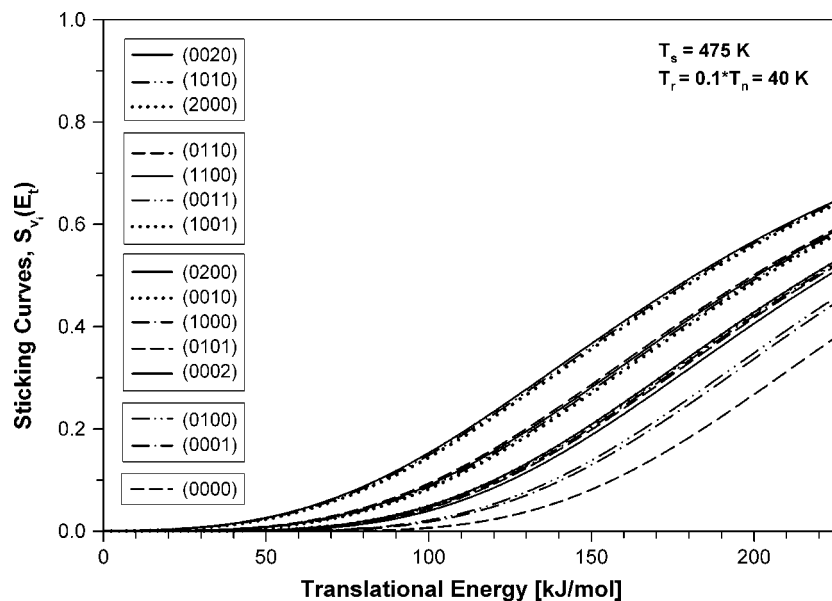


FIG. 7. PC-MURT predictions of the $S_{v_i}(E_t)$ vibrationaly resolved sticking curves for $T_n = 400$ K and $T_s = 475$ K.

to model conventional molecular beam experiments probing CH_4 dissociative chemisorption on Ni(100) in which the CH_4 vibrational state distribution was modulated by varying the beam's nozzle temperature. The $S_{v_i}(E_t)$ erf sticking ansatz as written in Eqs. (16) and employed in Eq. (14) has seen increasing use in modeling methane dissociative chemisorption^{5,11,13,14,17,59} and its inverse, methyl radical hydrogenation.²⁷ In these studies, Eq. (14) was used as a flexible form that admits the possibility of state selective reactivity through the erf form of $S_{v_i}(E_t)$ that has several free parameters. An experimental difficulty with conventional molecular beams with variable temperature nozzles is that the relative contributions to the observable net dissociative sticking from the many different vibrational states are expected to vary strongly with the beam translational energy (e.g., Figs. 5 and 6) and the nozzle temperature (e.g., Fig. 5 inset).

Fig. 1(ii)(c) & (d) reproduce the Holmblad *et al.*¹¹ molecular beam measurements of the variation of the $\text{CH}_4/\text{Ni}(100)$ dissociative sticking as a function of T_n . To employ the erf $S_{v_i}(E_t)$ curves in Eq. (14) to fit their variable T_n sticking data, Holmblad *et al.* made the simplifying assumption that only the C-H stretching modes were active in CH_4 dissociative chemisorption and modeled the molecules

as having only a single vibrational mode, a fourfold degenerate C-H stretch. Given their nozzle temperature range of 625 K–980 K, they reasoned that only the “ ν_3 ” = 0, 1, 2 states would be sufficiently thermally populated to be important contributors to the overall sticking. Further assuming $A_{v_i} = 1$ in the Eq. (16) erf form of $S_{v_i}(E_t)$, Holmblad *et al.* arrived at a six free parameter model. These free $S_{v_i}(E_t)$ parameters were fixed by fitting the variable T_n sticking data of Fig. 1(ii)(c) using Eq. (14) and are listed in Table I. When Holmblad *et al.* employed their six-parameter model to predict the dissociative sticking of CH_4 in thermal equilibrium high pressure bulb experiments⁶⁰ the agreement with experiment was encouragingly good. Their model predicts that molecules in the $\nu_3 = 1$ vibrationally excited state should dominate the thermal sticking. More recently, the eigenstate-resolved dissociative sticking of CH_4 ($1\nu_3, J=2$) on Ni(100) was found to be badly overestimated (e.g., ARD $\sim 4600\%$ in Fig. 8) using the Holmblad $S_{(0010)}(E_t)$ erf parameters and this was taken as evidence that vibrationally excited modes other than just ν_3 must substantially contribute to the CH_4 dissociative chemisorption in both thermal molecular beam and thermal bulb experiments.³

Schmid *et al.*⁵ used the erf form of $S_{v_i}(E_t)$ to directly fit their ($2\nu_3, J=2$) eigenstate-resolved and thermal molecular

TABLE I. Best fit parameters used in erf form of $S_{v_i}(E_t)$ and ARD comparison to PC-MURT $S_{v_i}(E_t)$ for molecular beam experiments with $T_r = 40$ K, $T_s = 475$ K, and $E_t \leq 150$ kJ/mol (see also Fig. 8).

Reference	Vibrational state ($\nu_1, \nu_2, \nu_3, \nu_4$)	A_{v_i}	E_{0,v_i} (kJ/mol)	W_{v_i} (kJ/mol)	ARD (%)
Holmblad <i>et al.</i>	(0000)	1.0	136.7	29.6	477
	(0010)	1.0	78.7	23.5	1.6×10^3
	(0020)	1.0	32.0	15.0	1.8×10^3
Schmid <i>et al.</i>	(0000)	0.0238	121.0	30.3	275
	(0020)	0.1128	63.0	28.3	75
Abbott <i>et al.</i> (this work)	(0000)	0.092	131.4	29.4	25
	(0010)	0.123	97.5	29.5	26
	(0020)	0.313	96.0	45.9	11

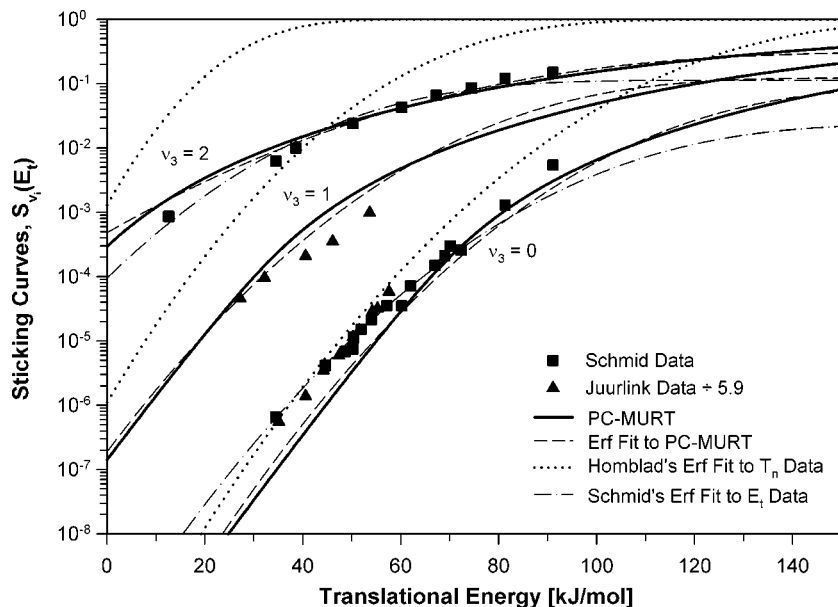


FIG. 8. PC-MURT predictions of the $S_{v_i}(E_t)$ vibrationally resolved sticking curves for 0, 1, and 2 quanta in the ν_3 antisymmetric C-H stretching mode are compared to optimized erf fits to these theoretical predictions and to various experimental data.

beam data of Fig. 1(i). They avoided the use of Eq. (14) to calculate the sticking as an average over different vibrational states and to average over the beam's translational energy distribution. The dissociative sticking from $T_n=400$ K thermal molecular beam was attributed entirely to CH_4 in the ground vibrational state. This may be a poor approximation because Fig. 6 predicts that the ground vibrational state contribution to the sticking varies from 35% to 80% over the 45 kJ/mol to 75 kJ/mol range of mean translational energy that they fitted. Within the PC-MURT, the $(2\nu_3, J=2)$ eigenstate-resolved molecular beam sticking can be calculated directly via Eq. (3), or along the lines of Eq. (14) without the need to average over different vibrational or rotational states,

$$\begin{aligned} S_{2\nu_3, J=2} &= S_{2\nu_3, J=2}(\langle E_t \rangle; T_t, T_s) \\ &= \int_0^\infty S_{2\nu_3, J=2}(E_t) f_t(E_t) dE_t, \end{aligned}$$

where

$$\begin{aligned} S_{2\nu_3, J=2}(E_t) &= \langle S(E_{2\nu_3}, E_{J=2}, E_t) \rangle_s \\ &= \int_0^\infty S(E_{2\nu_3} + E_{J=2} + E_t + E_s) f_s(E_s) dE_s. \end{aligned}$$

Clearly such eigenstate-resolved molecular beam sticking data are subject to relatively little averaging and are well suited for testing theoretical ideas. The Schmid *et al.* best fit erf $S_{v_i}(E_t)$ parameters for the (0000) and (0020) states are listed in Table I.

Given the long standing practice of fitting CH_4 molecular beam sticking using the erf $S_{v_i}(E_t)$ functional form, particularly for states involving the ν_3 antisymmetric C-H stretching mode, it is worth exploring if the erf form can be used to adequately represent $S_{v_i}(E_t)$ calculated by the PC-MURT using Eq. (15), especially if there is hope of gaining some insight as to the physical significance of the erf fitting parameters. Accordingly, Fig. 8 contrasts the $S_{v_i}(E_t)$ predic-

tions of the PC-MURT for the (0000), (0010), and (0020) vibrational states of CH_4 with our best erf $S_{v_i}(E_t)$ fits to these predictions and to the erf $S_{v_i}(E_t)$ curves reported by Holmblad *et al.*¹¹ and Schmid *et al.*⁵ Parameters for all the different erf $S_{v_i}(E_t)$ curves appear in Table I, along with the ARD between the erf and the PC-MURT $S_{v_i}(E_t)$ curves. The three PC-MURT $S_{v_i}(E_t)$ curves could be closely fitted using the erf $S_{v_i}(E_t)$ functional form to achieve ARDs in the 11%–26% range. The resulting erf fitting parameters do not appear to bear any obvious relationships to physical parameters of the reacting $\text{CH}_4/\text{Ni}(100)$ system such as the threshold energy for dissociative chemisorption, $E_0=65$ kJ/mol, or vibrational energy quanta. The Schmid erf $S_{v_i}(E_t)$ fits to the $(2\nu_3, J=2)$ eigenstate-resolved and thermal molecular beam sticking can be seen to represent the experimental data very well. Interestingly, Table I shows that the Schmid and PC-MURT erf $S_{v_i}(E_t)$ parameters for the (0020) vibrational state are surprisingly different given that both erf $S_{v_i}(E_t)$ curves provide a good representation of the $(2\nu_3, J=2)$ eigenstate-resolved experimental data. The PC-MURT $S_{v_i}(E_t)$ curve for the (0000) vibrational ground state lies beneath the $T_n=400$ K thermal molecular beam sticking data in Fig. 8 as expected based on Fig. 6 that indicates that the ground state contributes only fractionally to the sticking of the thermal beam. The erf $S_{v_i}(E_t)$ curves reported by Holmblad differed considerably from all the PC-MURT $S_{v_i}(E_t)$ curves, and from the erf $S_{v_i}(E_t)$ curves of Schmid. Ultimately, we are not able to attribute any special physical significance to the experimentally derived erf $S_{v_i}(E_t)$ fitting parameters. This is unfortunate because Schmid *et al.*⁵ use the centerpoint energies, $E_{0,(0020)}$ and $E_{0,(0000)}$, of their erf fittings to calculate a type of vibrational efficacy factor suggested by Luntz¹⁴ that they claim is relevant to whether the dissociative chemisorption dynamics are statistical or mode selective. Based on Fig. 8 and Table I, it appears that this kind of vibrational efficacy analysis based on erf fitting pa-

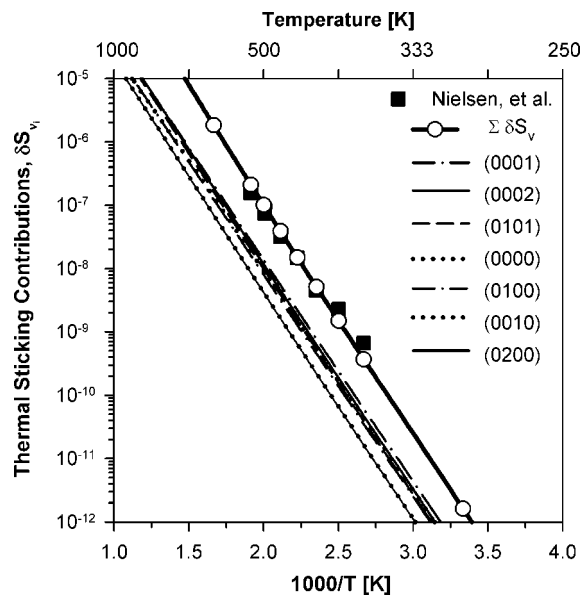


FIG. 9. PC-MURT prediction of some of the most important vibrationally resolved sticking contributions to the thermal equilibrium bulb experiments of Fig. 1(iii). The thermal sticking is dominated by methane in vibrationally excited states, particularly those involving excitation of the ν_4 bending mode. The order of vibrational states in the legend reflects the importance of their contributions to the sticking at 500 K (see also Table II).

rameters is difficult to experimentally implement with precision and cannot be theoretically justified based on the PC-MURT.

IV. VIBRATIONAL STATE RESOLVED DISSOCIATIVE STICKING FROM AN AMBIENT GAS AT THERMAL EQUILIBRIUM WITH A SURFACE

The formalism defined in Eqs. (14) and (15) for calculating vibrational state resolved dissociative sticking from molecular beams is easily adapted to the case of sticking

under thermal equilibrium conditions where an ambient gas impinges on a surface sharing a common temperature. The changes required are only to set all the temperatures equal (e.g., $T=T_t=T_v=T_r=T_s$) and to recognize that the angle integrated, flux-weighted, normal translational energy distribution,

$$f_t(E_t) = \frac{1}{k_b T} \exp\left(\frac{-E_t}{k_b T}\right) \quad (17)$$

for molecules striking a surface at thermal equilibrium should be used in Eq. (15).²⁸ Note that here we continue in our tradition, initiated after Eq. (5), of using E_t and “translational energy” as shorthand for $E_n = E_t \cos^2 \vartheta$ and “normal translational energy” (i.e., we’ve set $E_t = E_n$ alone).

An Arrhenius plot of the $\text{CH}_4/\text{Ni}(100)$ thermal dissociative sticking coefficient, S_T , along with its breakdown into contributions from the seven most important vibrational states is given in Fig. 9. Vibrational states with excited bending modes dominate the sticking at all the temperatures illustrated. The slopes of the δS_{v_i} versus $1000/T$ curves can be seen to vary somewhat with vibrational state. Because no one vibrational state has a fractional contribution to the overall sticking greater than 25%, it takes the contributions from a great many vibrational states to sum to even just 95% of the total experimental sticking. For example, summing the contributions from the first 47 vibrational states is required to recover 95% of the thermal sticking coefficient at 100 K, 1435 vibrational states are required at 1000 K.

Figure 10 shows the fractional contributions to the thermal sticking from the first 15 vibrational states plotted against temperature. Table II provides a listing of the various parameters relevant to calculating the vibrational state resolved contributions to the thermal sticking at 500 K, a temperature on the low side of the 500–1500 K range most relevant to industrial catalytic processes but one that remains

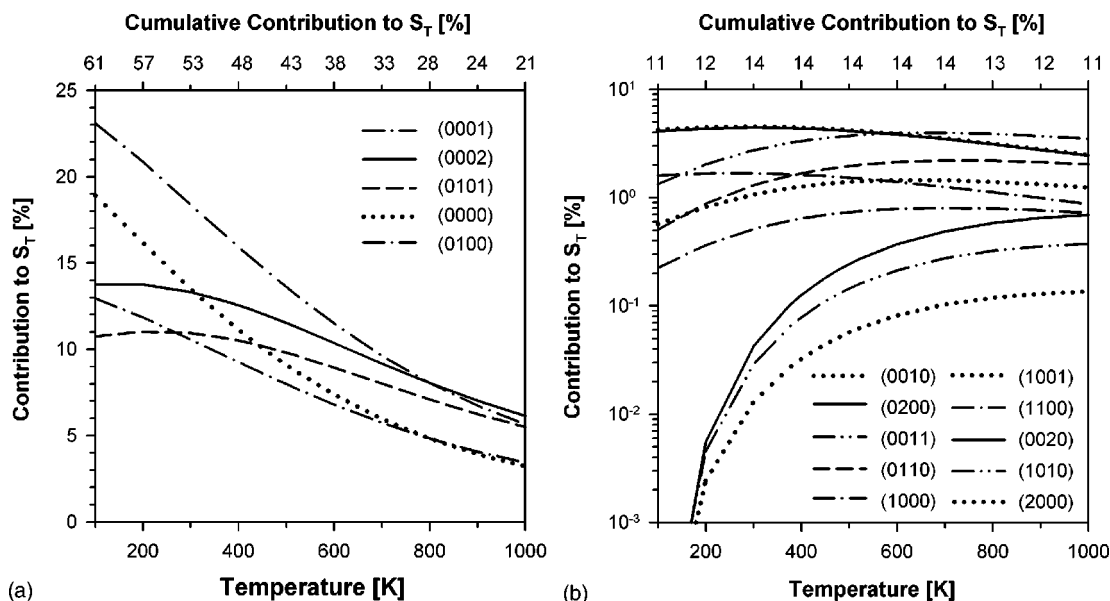


FIG. 10. PC-MURT predictions of the fractional contributions to the thermal sticking of Fig. 1(iii) from the first 15 vibrational states in energy. As the cumulative contributions on the upper x axes indicate, these 15 vibrational states account for less than 75% of the overall thermal sticking. The order of vibrational states in the legends reflects the importance of their contributions to the sticking at 500 K (see also Table II).

TABLE II. Vibrational state resolved dissociative sticking under thermal equilibrium conditions for 0, 1, and 2 vibrational quanta at 500 K [see also Figs. 9, 10, and 12(c)], $S_{T=500\text{ K}}=1.01\times 10^{-7}$.

Vibrational state ($\nu_1, \nu_2, \nu_3, \nu_4$)	g_{ν_i}	Energy (cm^{-1})	Maxwell-Boltzmann probability, P_{ν_i} (%)	S_{ν_i}	Contribution to thermal sticking (%)
(0000)	1	0	90.75	1.01×10^{-8}	9.09
(0001)	3	1305	6.37	2.16×10^{-7}	13.60
(0100)	2	1520	2.29	3.52×10^{-7}	7.97
(0002)	6	2610	0.30	3.91×10^{-6}	11.52
(0101)	6	2825	0.16	6.17×10^{-6}	9.79
(1000)	1	2915	2.06×10^{-2}	7.45×10^{-6}	1.52
(0010)	3	3020	4.58×10^{-2}	9.27×10^{-6}	4.20
(0200)	3	3040	4.32×10^{-2}	9.66×10^{-6}	4.13
(1001)	3	4220	1.45×10^{-3}	9.71×10^{-5}	1.39
(0011)	9	4325	3.21×10^{-3}	1.17×10^{-4}	3.73
(1100)	2	4435	5.20×10^{-4}	1.43×10^{-4}	0.73
(0110)	6	4540	1.15×10^{-3}	1.71×10^{-4}	1.96
(2000)	1	5830	4.70×10^{-6}	1.22×10^{-3}	0.06
(1010)	3	5935	1.04×10^{-5}	1.40×10^{-3}	0.14
(0020)	6	6040	1.54×10^{-5}	1.60×10^{-3}	0.24

easily accessible using surface science techniques. The cumulative contribution from the first 15 vibrational states at 500 K is 57% of the total S_T . The vibrational state resolved sticking coefficients, S_{ν_i} , can be seen to rise rapidly with vibrational energy but the Maxwell-Boltzmann weighting factors P_{ν_i} fall off even faster. As can be seen in Table II and Fig. 10, the optimal compromise between S_{ν_i} and P_{ν_i} is struck for the (0001) and (0002) vibrational states which contribute most to the overall thermal sticking. These states based on ν_4 bending mode excitations have relatively high degeneracy and low excitation energy. Other vibrational states built off ν_2 and ν_4 bending mode excitations, along with the vibrational ground state, are also important contributors to the thermal sticking. The C-H stretching modes contribute more modestly to the sticking with the (0010) state contributing 4.2% and ranking sixth in importance and the (1000) state contributing 1.5% and ranking tenth in importance at 500 K.

The mean normal translational energy for molecules striking the surface at thermal equilibrium is $\langle E_t \rangle = k_b T$. At 1000 K, $\langle E_t \rangle = 8.3$ kJ/mol which is towards the low end of the translational energies typically examined in molecular beam sticking experiments. Figure 6 shows a different ordering of the vibrational states contributing most to the molecular beam sticking at $E_t = 10$ kJ/mol as compared to the vibrational states contributing most to the thermal sticking at 1000 K in Fig. 10. For example, the (0001) state dominates the molecular beam sticking while the (0002) state dominates the thermal sticking. These differences arise simply because of the nonequilibrium nature of the molecular beam experiment where the temperatures of the surface $T_s = 475$ K, vibrations $T_v = T_n = 400$ K, and rotations $T_r = 0.1 T_n = 40$ K, all severely lag their counterparts in the $T = 1000$ K thermal equilibrium comparison experiment.

Although vibrational state resolved sticking information is available through molecular beam experiments employing variable temperature nozzles or direct laser pumping of single vibrational eigenstates, it has remained difficult to directly evaluate the contribution of rotational energy to the

dissociative chemisorption dynamics because the rotational degrees of freedom are largely frozen out by strong rotational cooling in the molecular beams.⁶¹ As shown in Figs. 5 and 6, conventional molecular beam experiments tend to be dominated by the sticking contribution from the vibrational ground state, promoted by the very high normal translational energies, as compared to sticking at thermal equilibrium where many more vibrational states make significant contributions to the sticking (e.g., Fig. 10). Consequently, conventional molecular beam experiments tend to report most directly on translational energy enhancement effects in activated dissociative chemisorption.

The PC-MURT assumes that rotational energy is fully active in the $\text{CH}_4/\text{Ni}(100)$ dissociative chemisorption and, based on the ($E_0 = 65$ kJ/mol, $\nu_D = 170$ cm^{-1} , $s = 2$) parameter set fixed by fitting the molecular beam experiments of Schmid *et al.*, manages to predict the thermal equilibrium sticking of Nielsen *et al.* very well (e.g., Fig. 1(iii) ARD = 33%). To determine which degrees of freedom are most important to dissociative chemisorption at thermal equilibrium, it is useful to calculate fractional energy uptakes defined as

$$f_j = \frac{\langle E_j \rangle_R}{\langle E^* \rangle_R}, \quad (18)$$

where $\langle E_j \rangle_R$ is the mean energy derived from the j th degrees of freedom of the molecules or surface oscillators forming physisorbed complexes that successfully react and $\langle E^* \rangle_R$ is the mean total energy of the successfully reacting physisorbed complexes.²⁸ Figure 11 illustrates how $\langle E_j \rangle_R$, $\langle E^* \rangle_R$, and the f_j 's vary with temperature under thermal equilibrium conditions. Also marked in Fig. 11(a) is the threshold energy for dissociation, $E_0 = 65$ kJ/mol, which is the thermal activation energy at 0 K according to the Tolman relation,

$$E_a = \langle E^* \rangle_R - \langle E^* \rangle, \quad (19)$$

where $\langle E^* \rangle$ is the mean total energy for all the physisorbed complexes formed. Figure 11 indicates that the energy re-

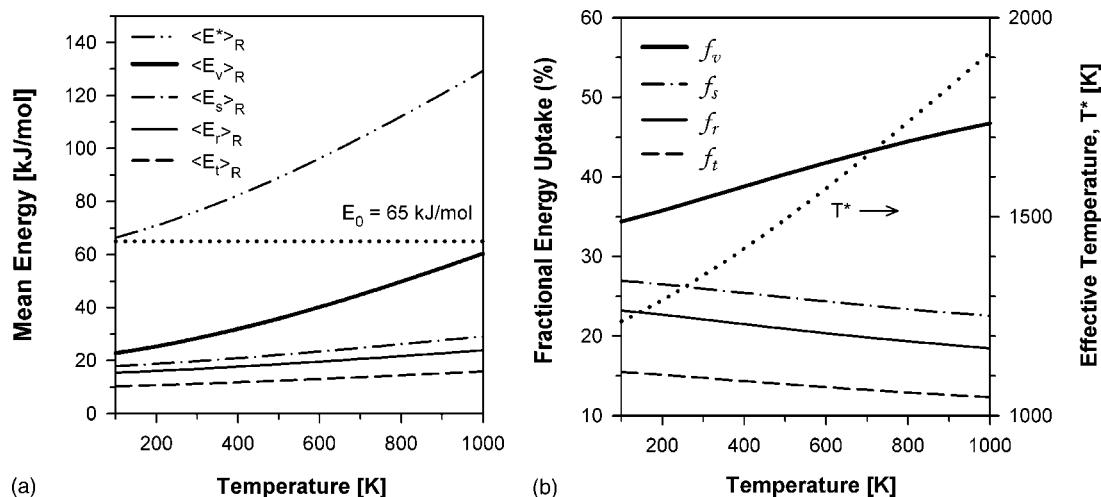


FIG. 11. PC-MURT predictions of (a) the mean energies of the reacting physisorbed complexes that derive from different gas and surface degrees of freedom, and (b) the fractional energy uptakes from the different degrees of freedom (e.g., $f_v = \langle E_v \rangle_R / \langle E^* \rangle_R$) and the effective temperature T^* of those species that successfully react. In thermal catalysis, about 75% of the energy required to surmount the barrier for dissociative chemisorption derives from the gas (i.e., $f_g = f_v + f_r + f_t \sim 75\%$).

quired to surmount the thermal activation barrier to dissociation derives primarily from the vibrational degrees of freedom, followed by the surface, rotational, and, finally, translational degrees of freedom. That molecular translation is the least important reactant degree of freedom in thermal dissociative chemisorption may be a counter-intuitive result based on familiarity with molecular beam experiments (e.g., Fig. 5). At 500 K, 75% of the total energy necessary for dissociative sticking derives from the gas with $f_t = 14\%$, $f_r = 21\%$, $f_v = 40\%$, and $f_s = 25\%$. Interestingly, there are relatively few experimental or theoretical studies that actively and explicitly explore the roles of the molecular rotational or surface degrees of freedom in dissociative chemisorption. The PC-MURT calculations of Fig. 11 suggest that under the thermal equilibrium conditions most relevant to catalysis both the rotational and surface degrees of freedom are vitally important.

Table III shows that the mean energies of the species that successfully react under thermal equilibrium at temperature $T = 500 \text{ K}$, $\langle E_j(T) \rangle_R$, closely resemble the energies for a thermal ensemble of species at a considerably higher temperature, $T^* = 1493 \text{ K}$. The variation of this “effective temperature” T^* descriptive of the reacting species at T as if they were a thermal ensemble at T^* is plotted along the right-hand axis of Fig. 11.

At thermal equilibrium, the energy distributions of the successfully reacting species deriving from the j th degrees of

freedom $f_{j,R}(E_j)$ of the gas or surface are easily calculated. For example, the translational energy distribution of the successfully reacting methane is

$$f_{t,R}(E_t) = \frac{S_t(E_t)f_t(E_t)}{\int_0^\infty S_t(E_t)f_t(E_t)dE_t} = \frac{S_t(E_t)f_t(E_t)}{S_T}, \quad (20)$$

where S_T is the thermal sticking coefficient, $f_t(E_t)$ is given by Eq. (17), and the thermal sticking coefficient for molecules with translational energy E_t is

$$S_t(E_t) = \langle S(E_t) \rangle_{rvs} = \int_0^\infty S(E_t + E_{rvs})f_{rvs}(E_{rvs})dE_{rvs}, \quad (21)$$

where

$$f_{rvs}(E_{rvs}) = \int_0^{E_{rvs}} f_r(E_r) \int_0^{E_{rvs}-E_r} f_v(E_v) \times f_s(E_{rvs}-E_v-E_r)dE_vdE_r. \quad (22)$$

For thermal dissociative chemisorption at $T = 500 \text{ K}$, Fig. 12 compares the reacting physisorbed complexes’ energy distributions deriving from different gas and surface degrees of freedom with the energy distributions for a thermal ensemble at an elevated effective temperature of $T^* = 1493 \text{ K}$. The reactive energy distributions are fairly well described by thermal distributions at an elevated effective

TABLE III. Energetics of the successfully reacting species under thermal equilibrium at $T = 500 \text{ K}$ compared to the energetics of a thermal ensemble of species at an effective temperature of $T^* = 1493 \text{ K}$ (see also Fig. 12).

Mode	f_j (%)	$\langle E_j(T) \rangle_R$ (kJ/mol) at $T = 500 \text{ K}$	$\langle E_j(T^*) \rangle$ (kJ/mol) at $T^* = 1493 \text{ K}$	
		$[\langle E^*(T) \rangle_R = 89 \text{ kJ/mol}]$	(kJ/mol)	$k_b T^*$
Translation, t	14	12.4	12.4	1.0
Rotation, r	21	18.6	18.6	1.5
Vibration, v	40	35.9	38.0	2.9
Surface, s	25	22.1	22.1	1.8

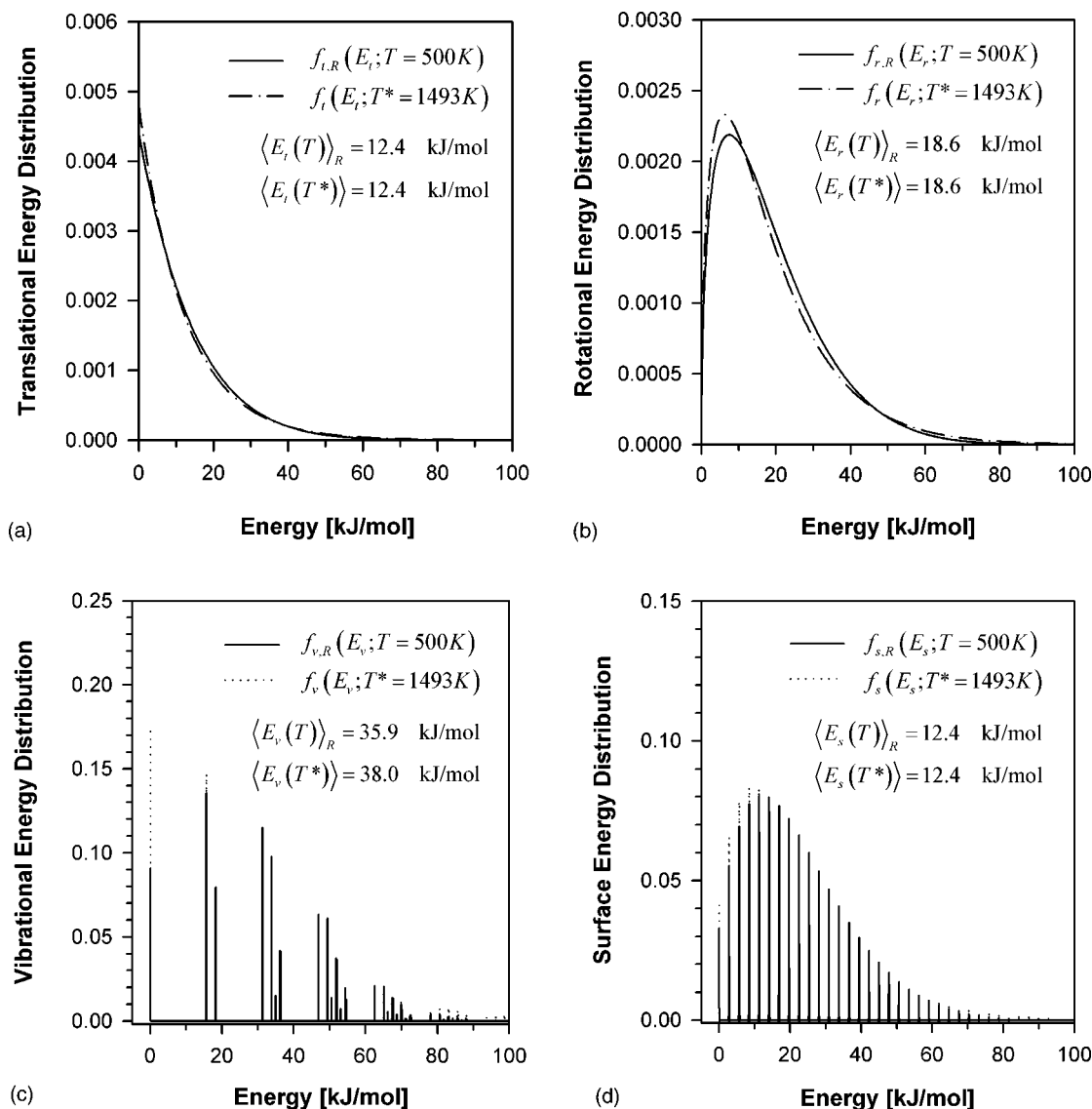


FIG. 12. For dissociative chemisorption at 500 K, the reacting physisorbed complexes' energy distributions deriving from different gas and surface degrees of freedom, $f_{j,R}(E_j; T=500\text{ K})$, are compared with the energy distributions, $f_j(E_j; T=1493\text{ K})$, for a thermal ensemble at 1493 K (see also Table III).

temperature, particularly, for the reactive distributions with quanta much smaller than $k_b T^*$ such that equipartition applies (see Table III). The reactive molecular vibrational energy distribution shows the most differences from a thermal distribution at T^* but this is not so surprising based on the large molecular vibrational quanta (e.g., $\nu_{\min} = \nu_4 = 1306\text{ cm}^{-1}$ or $T_{\nu_4} = 1879\text{ K}$) and hence relatively choppy interaction between $f_v(E_v; T=500\text{ K})$ and $S_\nu(E_\nu)$ as $f_{v,R}(E_v; T=500\text{ K})$ is calculated similarly to Eq. (20). Nevertheless, Fig. 12 shows that the simple description of the reacting species as a thermal ensemble with an elevated effective temperature is fairly accurate at 500 K.

By detailed balance, the energy distributions of Fig. 12 are the CH_4 product state distributions predicted for thermal CH_3 radical hydrogenation on Ni(100) at 500 K in the limit of zero coverage and no side reactions.^{25,62,63} Unfortunately, there are side reactions on Ni surfaces and adsorbed CH_3 radicals thermally decompose upon heating in the zero coverage limit.⁶⁴

V. DISCUSSION

A three-parameter formulation of the PC-MURT applied to the $\text{CH}_4/\text{Pt}(111)$ (Refs. 25 and 28) and $\text{CH}_4/\text{Ni}(100)$ (Refs. 21 and 56) dissociative chemisorption systems has been able to quantitatively predict a varied set of nonequilibrium molecular beam and thermal equilibrium high pressure bulb sticking experiments. The PC-MURT parameters of ($E_0 = 59\text{ kJ/mol}$, $\nu_D = 110\text{ cm}^{-1}$, $s = 3$) for $\text{CH}_4/\text{Pt}(111)$ define a 16 active degrees of freedom model²⁸ and the ($E_0 = 65\text{ kJ/mol}$, $\nu_D = 170\text{ cm}^{-1}$, $s = 2$) parameters for $\text{CH}_4/\text{Ni}(100)$ define a 15 degrees of freedom model.²¹ Alternative quantum dynamical models of methane dissociative chemisorption have treated 4 degrees of freedom or less. Such reduced dimensionality modeling has typically led to qualitative, rather than quantitative, theoretical predictions of experimental results. Early three dimensional (3D) quantum dynamical models include a thermally assisted tunneling theory²³ that treated methane as a quasidiatomic molecule,

R-H, and semiclassically incorporated a surface oscillator using a surface mass model.⁶⁵ A 3D multiconfiguration time-dependent Hartree model⁶⁶ kept the surface rigid and treated the R-H bond length, distance from the surface, and one orientation angle of the incident R-H “methane.” To simulate the effects of a higher-dimensional potential energy surface, Luntz semiempirically extended the thermally assisted tunneling model by first introducing a Gaussian distribution of reaction threshold energies²⁶ and, later, an additional Gaussian distribution of energy transfers with the surface.¹⁴ Recently, Carré and Jackson²⁰ and Zhang and co-workers⁶⁷ made 4D quantum simulations of CH₄ dissociative chemisorption on Ni(111) that included two molecular orientation angles to better explore the reactivity of different methane rotational states. Jackson’s work additionally accounted for surface temperature effects through the surface mass model.⁶⁵ These 4D quantum simulations on R-H methane claim qualitative agreement with Holmblad’s decomposition of the thermal molecular beam sticking of CH₄ on Ni(100) into erf $S_{v_i}(E_t)$ sticking curves for $v_3 = 0, 1, \text{ and } 2$. However, as was concluded earlier by Juurlink *et al.*,³ the Holmblad $S_{v_i}(E_t)$ curves for the v_3 states are only approximate (see Fig. 8) because sticking contributions from many more states are important to thermal beam sticking experiments as can be seen explicitly in the PC-MURT δS_{v_i} predictions of Figs. 5 and 6. Even for the most sophisticated 4D quantum simulations of methane dissociative chemisorption by Carré and Jackson, qualitative agreement with experiment is sometimes lacking. For example, a very much smaller kinetic isotope effect is theoretically predicted than is observed in Fig. 1(ii)(a) and predictions of rotational state selective sticking (i.e., very large variations in sticking with J) are not consistent with eigenstate-resolved experiments.⁶¹ Unfortunately, increasing the dimensionality of the quantum dynamics simulations to the full 15 degrees of freedom the PC-MURT employs for the CH₄/Ni(100) dissociative chemisorption is not computationally feasible at this time.

Ten dimensional quantum wave packet simulations of the inelastic scattering of methane from a flat rigid surface⁶⁸ for three specific collision orientations found that vibrational excitation of the incident methane enhanced translational to vibrational energy transfer with an efficiency that scales as $v_1 > v_3 > v_4 > \text{ground state}$. Without performing additional calculations admitting the possibility of dissociative chemisorption (i.e., their potential had no reactive exit channel), Milot and Jansen¹⁸ argued that vibrational state resolved dissociative sticking coefficients should scale with this efficiency of translational to vibrational energy transfer. They suggested that methane dissociative chemisorption should be mode selective with $S_{(1000)} > S_{(0010)} > S_{(0001)} > S_{(0000)}$ (n.b., $E_{(1000)} \approx E_{(0010)}$). In other work hinting that v_1 mode excitation might promote dissociation more efficiently than v_3 excitation, Halonen *et al.*¹⁹ performed 4D variational calculations to diagonalize the methane normal modes as the molecule approaches the surface and is perturbed by a surface potential similar to the one described by Carré and Jackson. When the molecule was brought as close as 2.2 Å from the surface, in the optimal orientation for dissociation ac-

ording to electronic structure theory calculations, the v_1 mode was found to correlate adiabatically to a localized oscillation of the C-H bond closest to the surface. By contrast, the v_3 mode was found to adiabatically correlate to C-H oscillations localized in the CH₃ group pointing away from the surface. To the extent that the reaction is vibrationally adiabatic these results suggest that excitation of the v_1 mode might be more effective than v_3 excitation because ultimately energy must be accumulated in the bond that breaks, namely, the C-H bond closest to the surface and not those within the CH₃ group pointing away from the surface. Analysis of Halonen *et al.* went further and considered the likelihood of vibrationally nonadiabatic processes on their model potential. They calculated a Massey velocity of $v_M = 1440 \text{ m/s}$ for the $v_1(A_1)/v_3(A_1)$ avoided crossing occurring 2.6 Å from the surface. This Massey velocity corresponds to a methane translational energy of 17 kJ/mol, on the low side of the translational energies examined by the molecular beam sticking experiments of Fig. 1. Given that adiabatic behavior should dominate if the molecular approach velocities are much smaller than v_M and vibrationally nonadiabatic behavior (i.e., hopping across adiabatic curves at avoided crossings) should dominate at velocities much greater than v_M , Halonen concluded that it is hard to justify either a fully adiabatic or a diabatic description of the vibrational dynamics of methane dissociative chemisorption. Of course, vibrationally nonadiabatic collision behavior near the surface would mix initially prepared vibrational states of methane and make mode specific chemistry unlikely to be observable. Both the Milot and Jansen¹⁸ and the Halonen *et al.*¹⁹ studies that were suggestive of mode specific chemistry examined only the entrance channel for CH₄ dissociative chemisorption and made no explicit calculations of dissociative sticking coefficients of any kind. Although vibrational state specific dissociation has been experimentally observed for CH₂D₂ on Ni(100),¹⁶ the vibrational mode nonspecific PC-MURT has sufficed to quantitatively predict the dissociative chemisorption behavior of CH₄ and CD₄ on Ni(100) as illustrated in Fig. 1.

Classical trajectory (molecular dynamics) simulations of methane dissociative chemisorption on Pd surfaces⁶⁹ find that translational energy is generally more effective than vibrational energy in activating methane towards dissociative chemisorption. In an analysis of nearly 150 trajectories, dissociation was best facilitated by different vibrational modes that depended on the methane orientation and collision site on the surface. Paavilainen and Nieminen⁶⁹ point out that considerable statistical averaging of classical trajectory calculations is required to make contact with experimental sticking coefficients. For example, Fig. 3 indicates that the number of open channels for desorption at the threshold energy for dissociative chemisorption, $W_D^\ddagger(E^* = E_0)$, for CH₄ on Ni(100) is more than 10⁶, a number representative of the number of possible initial conditions for classical trajectories of dissociative chemisorption. All of these trajectories at $E^* = E_0$ would have equal Boltzmann weighting in a simulation of sticking at thermal equilibrium. The trajectory study of Paavilainen and Nieminen found that dissociative sticking is activated by both bending and stretching vibrations. For

the CH_4/Pd molecular beam experiments, they qualitatively argued that bending excitations are most important to the sticking at low nozzle temperatures while stretching excitations become increasingly important at higher nozzle temperatures.

As can be seen in Fig. 1(iv), a specification of even the major distinguishing feature of the reactive potential energy surface for $\text{CH}_4/\text{Ni}(100)$, the threshold energy for dissociation, E_0 , has been a difficult problem for electronic structure theory. Given that dynamical theories require chemically accurate potential energy surfaces to quantitatively predict dissociative sticking coefficients or to assess and model the coupling and energy flow between vibrational modes near the transition state it is difficult to use the results of dynamical studies to justify the use of either the PC-MURT or the flexible erf $S_{v_i}(E_t)$ fitting approach¹⁴ to modeling experiments. Nevertheless, the latter two approaches have been the ones most successfully applied to experiments to date and we shall contrast them briefly below.

Figure 8 shows that a three-parameter Eq. (16) erf $S_{v_i}(E_t)$ fit to the $(2\nu_3, J=2)$ rovibrational eigenstate-resolved molecular beam data of Schmid *et al.* can provide an accurate representation of eigenstate-resolved sticking data. Unfortunately, neither Holmblad's procedure of fitting thermal molecular beam data using Eq. (14) and including erf $S_{v_i}(E_t)$ curves from only a small number of vibrational states (e.g., $\nu_3=0, 1, 2$) nor Schmid's procedure assuming sticking in thermal beams derives entirely from the vibrational ground state, provides an accurate description of the $S_{v_i}(E_t)$ curve for the vibrational ground state according to the PC-MURT calculations of Fig. 8. As discussed above, the PC-MURT further indicates that to accurately describe the thermal equilibrium sticking coefficient relevant to catalysis at 1000 K via Eq. (14) would require evaluation of three-parameter erf $S_{v_i}(E_t)$ curves for more than 1400 different vibrational states—a task that would require a great many state-of-the-art eigenstate-resolved molecular beam experiments to fix some 4200 free parameters. The erf fitting parameters are functions of the surface temperature according to Eq. (16) and would need to be reevaluated for each thermal temperature and methane isotope of interest [and possibly rotational state as well according to Eq. (1)]. There appears to be no physical significance that can be currently ascribed to the erf parameters (see Table II), primarily because the erf fitting procedure and parameters have never been rigorously derived from theory.¹⁴ Consequently, having a set of erf $S_{v_i}(E_t)$ parameters for a single rovibrational eigenstate at a specific T_s provides no insight as to what the erf parameters might be for another eigenstate, T_s , or isotope. Nor do the erf $S_{v_i}(E_t)$ parameters provide any insight as to features of the reactive potential energy surface for dissociative chemisorption.

In contrast, after the three parameters of the PC-MURT for $\text{CH}_4/\text{Ni}(100)$ were fixed by fitting the Schmid *et al.* data of Fig. 1(i), it was possible to quantitatively predict all the other varied experiments of Fig. 1 and provide a clear and quantitative connection between the results of experiment and electronic structure theory calculations (i.e., determine

the reaction threshold energy, E_0).²¹ Indeed, after once fixing the PC-MURT parameters, the theory makes definite predictions about the outcome of any conceivable dissociative sticking experiment, even ones with full quantum state resolution. As discussed above, the PC-MURT in its three-parameter formulation assumes that methane at the transition state has the same intramolecular vibrational frequencies as gas-phase methane, and that the three frustrated rotations and the molecular vibration normal to the surface at the transition state can be approximated as vibrating at the same low frequency, ν_D . As electronic structure theory at surfaces improves, it may be possible to accurately calculate all 12 of these transition state frequencies and E_0 directly. This would leave only the number of surface oscillators, s , effectively a dynamical energy exchange parameter, to be determined by experiments in order to complete the specification of a one parameter PC-MURT. Conversely, with sufficient input from state-resolved sticking experiments it might be possible to fix a (E_0 , 12 transition state frequencies, s) 14-parameter PC-MURT that would better define the potential energy surface at the transition state as a benchmark for electronic structure theory calculations. However, the fact that a three-parameter PC-MURT can predict all the varied experiments of Fig. 1 suggests that currently available experimental information is insufficient to justify a theoretical model with more parametrization.

Given the theoretically transparent formulation of the three-parameter PC-MURT, the prescription for making sticking coefficient predictions for other methane isotopomers based on a CH_4 parameter set is straightforward. For example, the E_0 barrier is adjusted according to the appropriate C-H(D) zero-point shift, ν_D is adjusted according to the isotopomer mass, and the desorption transition state at infinity is adjusted according to the gas-phase spectroscopy of the isotopomer.

Assuming that the three-parameter PC-MURT is capturing the essential chemical physics of the dissociative chemisorption of CH_4 on $\text{Ni}(100)$, what has our modeling revealed? Most importantly, the reaction appears to occur statistically [i.e., Eq. (4)] and is mode nonspecific such that the microcanonical sticking coefficient is a function of energy alone. Consequently, there can be no Polanyi rules⁷⁰ for this high dimensional reactive system that might relate preferential reactivity by translational energy to an early barrier on the potential energy surface and preferential reactivity by vibrational excitation to a late barrier on the potential energy surface. The fractional energy uptakes calculated in Fig. 11 for dissociative chemisorption under thermal equilibrium conditions remain interesting to consider. Over the temperature range from 500 K to 1500 K relevant to thermal catalysis, the incident gas-phase molecules supply the preponderance of energy used to surmount the barrier to dissociative chemisorption, $f_g = f_t + f_r + f_v \approx 75\%$, with the highest energy uptake always coming from the molecular vibrational degrees of freedom. Perhaps surprisingly, molecular rotational energy is predicted to be more important than translational energy in overcoming the thermal activation energy.

Ceyer has pointed out that when gas-phase molecules, and not the surface, supply most of the energy required to

overcome the barrier for an activated surface process a “pressure gap” may exist between the results of thermal catalysis and ultrahigh vacuum (UHV) surface science.²⁴ The problem is that high energy gas-surface collisions from the tail of the Boltzmann distribution are repetitively sampled under the high pressure conditions of catalysis while under UHV with thermal gas dosing there is typically only a single collision with the surface. Under UHV if the molecule non-dissociatively sticks then upon heating the molecule is much more likely to desorb than to react. In this paper we have shown that molecular beam experiments informing the PC-MURT can bridge the pressure gap and provide accurate predictions about thermal dissociative sticking coefficients relevant to catalysis. Under thermal equilibrium conditions at temperature T , Table III and Figs. 11 and 12 indicate that the successfully reacting species have an energy distribution that can be reasonably well described by a thermal distribution at a considerably higher effective temperature T^* . In other words, the successfully reacting species have a much higher effective temperature than their surroundings—an idea consistent with our development of the PC-MURT as a local hot spot model for gas-surface reactivity.

VI. SUMMARY

The predictions of a simple, three-parameter microcanonical theory of gas-surface reactivity, the PC-MURT, were shown to be quantitatively consistent with varied nonequilibrium molecular beam^{3,5,11} and thermal equilibrium high pressure bulb¹⁵ experiments, as well as *ab initio* quantum chemistry calculations indicating the reaction threshold energy is $E_0 = 67 \pm 4$ kJ/mol,⁵⁷ for CH₄ dissociative chemisorption on Ni(100). The PC-MURT was used to predict vibrational state resolved contributions to the dissociative sticking of CH₄ on Ni(100) and the results were compared to those of other dynamical theories and currently available experimental data. For the activated dissociative chemisorption at thermal equilibrium, the successfully reacting species (i.e., physisorbed complexes composed of a molecule + a few local surface oscillators) were predicted to have a much higher effective temperature than their surroundings, with about 75% of their energy deriving from molecular degrees of freedom.

ACKNOWLEDGMENT

This research was supported by the National Science Foundation (NSF), Grant No. 0078995, and by the donors of the American Chemical Society Petroleum Research Fund. H.L.A. and A.B. gratefully acknowledge fellowship support under NSF IGERT Grant No. 9972790. We thank Arthur Utz for helpful discussions that motivated this work and Rainer Beck for providing extended and updated experimental data prior to its publication elsewhere.

¹G. O. Sitz, Rep. Prog. Phys. **65**, 1165 (2002).

²A. C. Luntz, Science **302**, 70 (2003).

³L. B. F. Juurlink, P. R. McCabe, R. R. Smith, C. L. DiCologero, and A. L. Utz, Phys. Rev. Lett. **83**, 868 (1999).

⁴J. Higgins, A. Conjusteau, G. Scoles, and S. L. Bernasek, J. Chem. Phys. **114**, 5277 (2001).

⁵M. P. Schmid, P. Maroni, R. D. Beck, and T. R. Rizzo, J. Chem. Phys. **117**, 8603 (2002); R. D. Beck (private communication).

- ⁶C. T. Rettner, D. J. Auerbach, and H. A. Michelsen, Phys. Rev. Lett. **68**, 1164 (1992).
- ⁷C. T. Rettner, H. A. Michelsen, and D. J. Auerbach, J. Chem. Phys. **102**, 4625 (1995).
- ⁸C. T. Rettner, H. E. Pfnur, and D. J. Auerbach, Phys. Rev. Lett. **54**, 2716 (1985).
- ⁹C. T. Rettner, H. E. Pfnur, and D. J. Auerbach, J. Chem. Phys. **84**, 4163 (1986).
- ¹⁰M. B. Lee, Q. Y. Yang, and S. T. Ceyer, J. Chem. Phys. **87**, 2724 (1987).
- ¹¹P. M. Holmblad, J. Wambach, and I. Chorkendorff, J. Chem. Phys. **102**, 8255 (1995).
- ¹²A. C. Luntz and D. S. Bethune, J. Chem. Phys. **90**, 1274 (1989).
- ¹³J. H. Larsen, P. M. Holmblad, and I. Chorkendorff, J. Chem. Phys. **110**, 2637 (1999).
- ¹⁴A. C. Luntz, J. Chem. Phys. **113**, 6901 (2000).
- ¹⁵B. O. Nielsen, A. C. Luntz, P. M. Holmblad, and I. Chorkendorff, Catal. Lett. **32**, 15 (1995).
- ¹⁶R. D. Beck, P. Maroni, D. C. Papageorgopoulos, T. T. Dang, M. P. Schmid, and T. R. Rizzo, Science **302**, 98 (2003).
- ¹⁷J. H. Larsen and I. Chorkendorff, Surf. Sci. Rep. **35**, 165 (1999).
- ¹⁸R. Milot and A. P. J. Jansen, Phys. Rev. B **61**, 15657 (2000).
- ¹⁹L. Halonen, S. L. Bernasek, and D. J. Nesbitt, J. Chem. Phys. **115**, 5611 (2001).
- ²⁰M. N. Carré and B. Jackson, J. Chem. Phys. **108**, 3722 (1998).
- ²¹H. L. Abbott, A. Bukoski, D. F. Kavulak, and I. Harrison, J. Chem. Phys. **119**, 6407 (2003).
- ²²H. F. Winters, J. Chem. Phys. **64**, 3495 (1976).
- ²³J. Harris, J. Simon, A. C. Luntz, C. B. Mullins, and C. T. Rettner, Phys. Rev. Lett. **67**, 652 (1991).
- ²⁴S. T. Ceyer, Science **249**, 133 (1990).
- ²⁵V. A. Ukraintsev and I. Harrison, J. Chem. Phys. **101**, 1564 (1994).
- ²⁶A. C. Luntz, J. Chem. Phys. **102**, 8264 (1995).
- ²⁷H. Mortensen, L. Diekhoner, A. Baurichter, and A. C. Luntz, J. Chem. Phys. **116**, 5781 (2002).
- ²⁸A. Bukoski, D. Blumling, and I. Harrison, J. Chem. Phys. **118**, 843 (2003).
- ²⁹C. T. Rettner, D. J. Auerbach, J. C. Tully, and A. W. Kleyn, J. Phys. Chem. **100**, 13021 (1996).
- ³⁰T. Baer and W. L. Hase, *Unimolecular Reaction Dynamics* (Oxford University Press, New York, NY, 1996).
- ³¹J. C. Keske and B. H. Pate, Annu. Rev. Phys. Chem. **51**, 323 (2000).
- ³²W. B. Miller, S. A. Safron, and D. R. Herschbach, Discuss. Faraday Soc. **44**, 108 (1967).
- ³³R. Grice, Int. Rev. Phys. Chem. **14**, 315 (1995).
- ³⁴L. Bonnet and J. C. Rayez, Phys. Chem. Chem. Phys. **1**, 2383 (1999).
- ³⁵P. A. Willis, H. U. Stauffer, R. Z. Hinrichs, and H. F. Davis, J. Phys. Chem. A **103**, 3706 (1999).
- ³⁶I. R. Sims, M. Gruebele, E. D. Potter, and A. H. Zewail, J. Chem. Phys. **97**, 4127 (1992).
- ³⁷J. J. Wang, D. J. Smith, and R. Grice, Chem. Phys. **207**, 203 (1996).
- ³⁸D. G. Schultz and L. Hanley, J. Chem. Phys. **109**, 10976 (1998).
- ³⁹K. Y. Song, O. Meroueh, and W. L. Hase, J. Chem. Phys. **118**, 2893 (2003).
- ⁴⁰C. T. Rettner, D. J. Auerbach, and H. A. Michelsen, Phys. Rev. Lett. **68**, 2547 (1992).
- ⁴¹A. Hodgson, J. Moryl, P. Traversaro, and H. Zhao, Nature (London) **356**, 501 (1992).
- ⁴²Z. S. Wang, G. R. Darling, and S. Holloway, J. Chem. Phys. **120**, 2923 (2004).
- ⁴³S. A. Egorov and J. L. Skinner, J. Chem. Phys. **103**, 1533 (1995).
- ⁴⁴D. L. Bunker and W. L. Hase, J. Chem. Phys. **59**, 4621 (1973).
- ⁴⁵K. Freed, Faraday Discuss. **67**, 231 (1979).
- ⁴⁶S. A. Reid and H. Reisler, J. Phys. Chem. **100**, 474 (1996).
- ⁴⁷R. Hernandez, W. H. Miller, C. B. Moore, and W. F. Polik, J. Chem. Phys. **99**, 950 (1993).
- ⁴⁸J. D. Tobiasson, J. R. Dunlop, and E. A. Rohlfing, J. Chem. Phys. **103**, 1448 (1995).
- ⁴⁹R. Marquardt, M. Quack, and I. Thanopoulos, J. Phys. Chem. A **104**, 6129 (2000).
- ⁵⁰C. G. Elles, D. Bingemann, M. M. Heckscher, and F. F. Crim, J. Chem. Phys. **118**, 5587 (2003).
- ⁵¹L. R. Brown, D. C. Benner, J. P. Champion *et al.*, J. Quant. Spectrosc. Radiat. Transf. **82**, 219 (2003).
- ⁵²X. G. Wang and E. L. Sibert, J. Chem. Phys. **111**, 4510 (1999).

- ⁵³Z. H. Kim, H. A. Bechtel, and R. N. Zare, *J. Am. Chem. Soc.* **123**, 12714 (2001).
- ⁵⁴S. Yoon, S. Henton, A. N. Zivkovic, and F. F. Crim, *J. Chem. Phys.* **116**, 10744 (2002).
- ⁵⁵Z. H. Kim, H. A. Bechtel, and R. N. Zare, *J. Chem. Phys.* **117**, 3232 (2002).
- ⁵⁶A. Bukoski and I. Harrison, *J. Chem. Phys.* **118**, 9762 (2003).
- ⁵⁷O. Swang, K. Faegri, O. Gropen, U. Wahlgren, and P. Siegbahn, *Chem. Phys.* **156**, 379 (1991).
- ⁵⁸A. L. Utz (private communication).
- ⁵⁹A. T. Gee, B. E. Hayden, C. Mormiche, A. W. Kleyn, and B. Riedmuller, *J. Chem. Phys.* **118**, 3334 (2003).
- ⁶⁰I. Chorkendorff, I. Alstrup, and S. Ullmann, *Surf. Sci.* **227**, 291 (1990).
- ⁶¹L. B. F. Juurlink, R. R. Smith, and A. L. Utz, *Faraday Discuss.* **117**, 147 (2000).
- ⁶²K. Watanabe, M. C. Lin, Y. A. Gruzdkov, and Y. Matsumoto, *J. Chem. Phys.* **104**, 5974 (1996).
- ⁶³I. Harrison, *Acc. Chem. Res.* **31**, 631 (1998).
- ⁶⁴Q. Y. Yang and S. T. Ceyer, *J. Vac. Sci. Technol. A* **6**, 851 (1988).
- ⁶⁵A. C. Luntz and J. Harris, *Surf. Sci.* **258**, 397 (1991).
- ⁶⁶A. P. J. Jansen and H. Burghgraef, *Surf. Sci.* **344**, 149 (1995).
- ⁶⁷Y. Xiang, J. Z. H. Zhang, and D. Y. Wang, *J. Chem. Phys.* **117**, 7698 (2002); Y. Xiang and J. Z. H. Zhang, *ibid.* **118**, 8954 (2003).
- ⁶⁸R. Milot and A. P. J. Jansen, *J. Chem. Phys.* **109**, 1966 (1998); R. Milot and A. P. J. Jansen, *Surf. Sci.* **452**, 179 (2000).
- ⁶⁹S. Paavilainen and J. A. Nieminen, *Phys. Rev. B* **66**, 155409 (2002).
- ⁷⁰J. C. Polanyi and W. H. Wong, *J. Chem. Phys.* **51**, 1439 (1969).
- ⁷¹T. P. Beebe, D. W. Goodman, B. D. Kay, and J. T. Yates, *J. Chem. Phys.* **87**, 2305 (1987).
- ⁷²R. C. Egeberg, S. Ullmann, I. Alstrup, C. B. Mullins, and I. Chorkendorff, *Surf. Sci.* **497**, 183 (2002).
- ⁷³A. B. Anderson and J. J. Maloney, *J. Phys. Chem.* **92**, 809 (1988).
- ⁷⁴H. Yang and J. L. Whitten, *J. Chem. Phys.* **96**, 5529 (1992).
- ⁷⁵H. Burghgraef, A. P. J. Jansen, and R. A. Vansanten, *J. Chem. Phys.* **101**, 11012 (1994).
- ⁷⁶P. Kratzer, B. Hammer, and J. K. Nørskov, *J. Chem. Phys.* **105**, 5595 (1996).
- ⁷⁷H. S. Bengaard, I. Alstrup, I. Chorkendorff, S. Ullmann, J. R. Rostrup-Nielsen, and J. K. Nørskov, *J. Catal.* **187**, 238 (1999).
- ⁷⁸V. Ledentu, W. Dong, and P. Sautet, *J. Am. Chem. Soc.* **122**, 1796 (2000).
- ⁷⁹H. S. Bengaard, J. K. Nørskov, J. Sehested, B. S. Clausen, L. P. Nielsen, A. M. Molenbroek, and J. R. Rostrup-Nielsen, *J. Catal.* **209**, 365 (2002).